FISEVIER

Contents lists available at ScienceDirect

Journal of Human Evolution

journal homepage: www.elsevier.com/locate/jhevol



A new species of fossil guenon (Cercopithecini, Cercopithecidae) from the Early Pleistocene Lower Ngaloba Beds, Laetoli, Tanzania



Julia L. Arenson ^{a, b, *}, Terry Harrison ^{b, c}, Eric J. Sargis ^{d, e, f}, Hannah G. Taboada ^c, Christopher C. Gilbert ^{a, b, g, h}

- ^a PhD Program in Anthropology, The Graduate Center of the City University of New York, 365 Fifth Avenue, New York, NY, 10016, USA
- ^b New York Consortium in Evolutionary Primatology (NYCEP), New York, NY, 10016, USA
- ^c Center for the Study of Human Origins, Department of Anthropology, New York University, 25 Waverly Place, New York, NY, 10003, USA
- ^d Department of Anthropology, Yale University, 10 Sachem Street, New Haven, CT, 06511, USA
- e Divisions of Vertebrate Paleontology and Vertebrate Zoology, Yale Peabody Museum of Natural History, 170 Whitney Avenue, New Haven, CT, 06511, USA
- f Yale Institute for Biospheric Studies, P.O. Box 208118, New Haven, CT, 06520, USA
- g Department of Anthropology, Hunter College, CUNY, 695 Park Avenue, New York, NY, 10065, USA
- ^h Division of Paleontology, American Museum of Natural History, Central Park West, New York, NY, 10024, USA

ARTICLE INFO

Article history: Received 10 August 2021 Accepted 6 December 2021 Available online xxx

Keywords: Chlorocebus Cercopithecus Cercopithecin Cranium Mandible Dentition

ABSTRACT

The living guenons (Cercopithecini, Cercopithecidae) are speciose and widely distributed across sub-Saharan Africa but are poorly represented in the fossil record. In addition, the craniodental and skeletal similarity of the guenons has hampered the identification of fragmentary material, likely obscuring the taxonomic diversity represented in the fossil record. Here, we describe a new fossil guenon specimen (LAET 75-3703) from the Lower Ngaloba Beds, Laetoli in Tanzania, dated to ~1.7-1.2 Ma and preserving the lower face and mandible. Comparison to 278 extant guenon specimens, representing all six extant genera, identified several informative traits for distinguishing between the morphologically similar Chlorocebus and Cercopithecus, and these support the attribution of LAET 75-3703 to Chlorocebus. A discriminant function analysis of seven craniodental indices on a subsample of Chlorocebus and Cercopithecus was robust with an overall correct classification rate of 80.4%, and it classified LAET 75-3703 as a member of Chlorocebus with a posterior probability of 92.7%. LAET 75-3703 shares with Chlorocebus the presence of small 'thumbprint' depressions on the maxilla; a tall, narrow, and diamond-shaped nasal aperture; a relatively longer and shallower face; relatively buccolingually broader molars; and a shallow mandible that decreases in depth posteriorly. In addition, LAET 75-3703 is distinguished from all extant guenons, including other species of Chlorocebus, in having a very small P³ relative to M¹ area. As such, LAET 75-3703 is assigned to a new species, Chlorocebus ngedere sp. nov. This specimen represents the first cercopithecin from Laetoli, as well as the oldest fossil cercopithecin confidently attributed to a modern genus.

© 2021 Elsevier Ltd. All rights reserved.

1. Introduction

1.1. The cercopithecin fossil record

The guenons (Cercopithecini, Cercopithecidae) are a diverse group of Old World monkeys distributed across sub-Saharan Africa comprising at least six genera: the diverse and largely arboreal Cercopithecus genus; the 'terrestrial clade' of patas monkeys

* Corresponding author.

E-mail address: arenson.jl@gmail.com (J.L. Arenson).

(Erythrocebus), vervets (Chlorocebus), and mountain monkeys (Allochrocebus); Allen's swamp monkey (Allenopithecus); and the diminutive talapoins (Miopithecus; Lernould, 1988; Butynski, 2002; Grubb et al., 2003; Butynski et al., 2013; Turner et al., 2019a). Of the living guenons, Cercopithecus and Chlorocebus are craniodentally similar and were considered congeneric until molecular studies demonstrated the arrangement was polyphyletic (Groves, 1989, 2001; Tosi et al., 2004, 2005; Xing et al., 2007). Uncertainty remains in the placement of Miopithecus and Allenopithecus and the relationships among the Cercopithecus species groups, with different molecular markers recovering alternative topologies (e.g., Tosi et al., 2002a, 2005; Xing et al., 2007; Perelman et al., 2011;

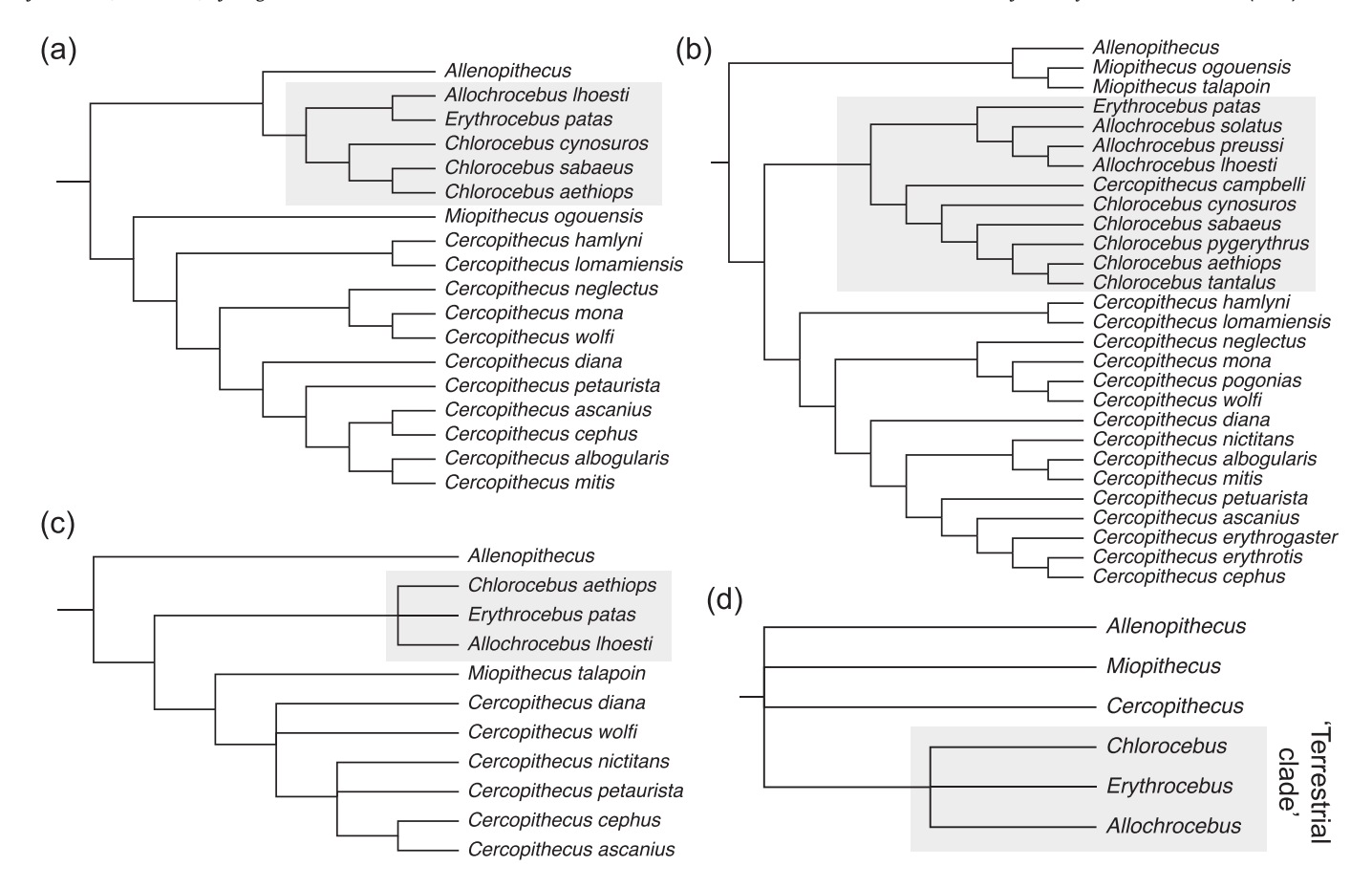


Figure 1. Recent molecular phylogenies of the guenons (a–c) and genus-level consensus tree (d). Phylogenies from a) Perelman et al. (2011) using nuclear DNA markers, b) Springer et al. (2012) using mitochondrial and nuclear DNA markers, and c) Xing et al. (2007) using Alu insertions. The monophyly of the 'terrestrial clade' (highlighted in gray) comprising Chlorocebus, Erythrocebus, and Allochrocebus is well supported. The position of Cercopithecus campbelli in (b) has not been replicated and is likely not indicative of its true phylogenetic position.

Springer et al., 2012). However, the monophyly of each genus, as well as the monophyly of the terrestrial clade, appears well supported (Fig. 1; Tosi et al., 2004; Xing et al., 2007; Perelman et al., 2011; Springer et al., 2012).

The evolutionary history of the guenons has remained poorly understood in part because of a scant fossil record (Leakey, 1988; Lo Bianco et al., 2017; Plavcan et al., 2019). Despite their current extant diversity and an estimated clade origin date in the Miocene ca. 12.3–9.8 Ma (Raaum et al., 2005; Steiper and Young, 2006; Fabre et al., 2009; Springer et al., 2012; Guschanski et al., 2013; Linden et al., 2020), the fossil record of the guenons is limited. Few specimens have been recovered from otherwise productive Plio-Pleistocene sites in eastern Africa (Eck and Howell, 1972; Eck, 1987; Leakey, 1988; Harrison and Harris, 1996; Frost and Alemseged, 2007; Jablonski et al., 2008; Jablonski and Frost, 2010; Plavcan et al., 2019; Frost et al., 2020) and Middle to Late Pleistocene sites in South Africa (Klein, 1977; Ogola, 2009; Mokokwe, 2016; Fig. 2; Supplementary Online Material [SOM] Table S1).

The oldest fossil attributed to the Cercopithecini is known from just outside continental Africa, represented by an isolated lower molar from Abu Dhabi dated to ~8–6 Ma (Gilbert et al., 2014). A large temporal and geographic gap persists after this fossil until the Early Pliocene of East Africa, where the diminutive talapoin-sized *Nanopithecus browni* is known from Kanapoi and Koobi Fora in Kenya, dating from 4.2 Ma to older than 3.4 Ma (Leakey, 1976, 1988;

Jablonski et al., 2008; Plavcan et al., 2019; Frost et al., 2020). Other Early Pliocene cercopithecins are less securely dated and even more fragmentary: fossils putatively considered to come from the Haradaso Member of the Sagantole Formation in the Middle Awash of Ethiopia might date to the Early Pliocene, but their exact provenance is unknown (Kalb et al., 1982a, b). A poorly preserved mandible of a juvenile individual from Kanam East in Kenya is possibly of Early Pliocene age, but again the stratigraphic provenance is uncertain (Szalay and Delson, 1979; Harrison and Harris, 1996).

In the Late Pliocene and Early Pleistocene, fragmentary dentognathic material is known from the Omo group in Ethiopia (Eck and Howell, 1972; Eck, 1987). A few isolated molars dated to 3.3 Ma and some mandibular fragments at 2.3 Ma show affinities with cercopithecins in the lack of a hypoconulid on the M₃ and in overall crown morphology (Eck and Howell, 1972; Eck, 1987). Comparisons showed that these fossils were most similar in size to male Cercopithecus nictitans but were similar in morphology to both Ce. nictitans and Chlorocebus (Eck and Howell, 1972; Eck, 1987). A Cercopithecus mitis-sized cercopithecin (Cercopithecus sp. A) is known from limited dental material and two postcranial elements from Koobi Fora in Kenya and is dated to the Early Pleistocene ca. 2.0-1.6 Ma (Jablonski et al., 2008). Much of this material is attributed either to Cercopithecus sp. indet. or to 'Cercopithecus aethiops' by virtue of its general cercopithecin affinities, but few specimens are adequately preserved or complete enough to allow a more

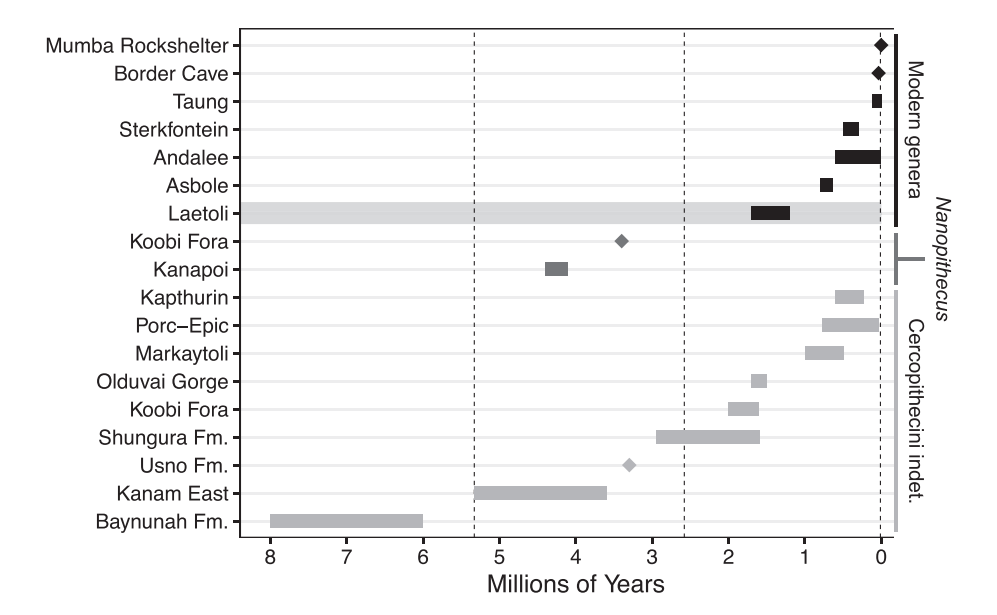


Figure 2. Distribution of material attributed to the tribe Cercopithecini through time. Bars represent age range estimates, and diamonds represent point estimates (or ranges less than 0.05 Ma). The vertical dashed lines mark epoch boundaries. Most material is attributed to Cercopithecini indet. (or *Cercopithecus* sp. as a marker of general cercopithecin affinity; see text for further discussion of taxonomic rearrangements within the guenons). *Nanopithecus* represents the only fossil guenon genus at ca. 4.4–3.4 Ma. At ~1.7–1.2 Ma, *Chlorocebus ngedere* (LAET 75-3703) is the oldest representative of a modern genus. See <u>SOM Table S1</u> for sources and specific dates.

confident generic or specific designation. Until more diagnostic material is known, this material should conservatively be considered Cercopithecini indet.

Younger material from the Pleistocene is better represented by large samples from the Afar Depression at the Middle Pleistocene sites of Asbole and Andalee, attributed to cf. Chlorocebus and cf. Erythrocebus (= cf. Chlorocebus aff. aethiops and cf. Chlorocebus cf. patas, respectively, in the studies by Kalb et al., 1982a; Alemseged and Geraads, 2000; Frost, 2001; Frost and Alemseged, 2007). More specific taxonomic identifications for the Asbole material are facilitated by their relative completeness (Frost, 2001; Frost and Alemseged, 2007). Cercopithecin specimens are also known from the Middle to Late Pleistocene at Olduvai Gorge and Mumba Rockshelter in Tanzania, Loboi and Kapthurin in Kenya, and Markaytoli and Porc-Epic in Ethiopia (Leakey, 1988; Alemseged and Geraads, 2000; Assefa, 2006; Prendergast et al., 2007; C.C.G., pers. obs.). In South Africa, Chlorocebus sp. is recorded from a Late Pleistocene site at Taung (Broadfield et al., 1994) and Middle and Late Pleistocene sites at Sterkfontein and Border Cave (Klein, 1977; Ogola, 2009; Mokokwe, 2016). Thus, the limited fossil record of Cercopithecini is principally known from the later Pleistocene and from sites in the northern portion of the East African Rift Valley.

To date, no cercopithecins have been reported from Laetoli, which has yielded a relative abundance of cercopithecid monkeys in the Upper Laetolil Beds (~3.8—3.5 Ma) and a few specimens from the Upper Ndolanya Beds (~2.66 Ma) and the Lower Laetolil Beds (~4.3—3.8 Ma; Leakey and Delson, 1987; Harrison, 2011; Laird et al., 2018; Reed et al., 2019). These belong to three papionin species (*Parapapio ado, Theropithecus oswaldi* ssp., and Papionini gen. et sp. indet.) and two colobine species (*Cercopithecoides* sp. and cf. *Rhinocolobus* sp.; Harrison, 2011; Frost et al., 2018). In addition, two dentognathic specimens of *Papio* sp. were recovered by Kohl-Larsen in 1939 from Laetoli at Lemagrut Korongo (Dietrich, 1942; Harrison, 2011), but their stratigraphic provenance is unknown. The preservation of these specimens and adhering matrix indicate that they are from Pleistocene sediments, possibly from the Ngaloba Beds.

Here we describe a partial skull of a cercopithecin (LAET 75-3703) recovered from the Early Pleistocene Lower Ngaloba Beds (LNB) at

Laetoli in northern Tanzania. The specimen was found in 1975 by teams directed by Mary Leakey, but it has remained undescribed until now. This is the first record of a cercopithecin from Laetoli and is one of the most complete specimens known from the Pleistocene of eastern Africa. LAET 75-3703 exhibits morphological features most consistent with *Chlorocebus* and represents the earliest known record of an extant cercopithecin genus (Fig. 2).

1.2. Geology and chronology

LAET 75-3703 was recovered from Laetoli Locality 1 (previously referred to as Olduvai Side Gorge or Marambu) in 1975 by a team led by Mary Leakey. The specimen was recovered from 'pink beds' in the LNB in association with other faunal remains and a number of flake artifacts. The LNB consist of alternating sandstones and conglomerates, with some claystones deposited in small channels cut into the underlying Laetolil Beds (Hay, 1987; Manega, 1993). Unfortunately, no datable tuffs have been identified in the LNB, so their age is poorly constrained by the dates of the Olpiro Beds (2.0 Ma) and the Upper Ngaloba Beds (~0.2 Ma; Drake and Curtis, 1978; Ndessokia, 1990; Manega, 1993; Deino, 2011). The LNB have yielded faunal remains and Acheulian tools consisting of large bifaces and choppers made of calcrete, lava, and basement rock (Kohl-Larsen, 1943; Harris and Harris, 1981; Leakey, 1987; Harrison and Kweka, 2011). The mammal fauna from the LNB includes T. oswaldi, Sivatherium maurusium, Pelorovis sp., Gazella sp., Hippopotamus gorgops, Kolpochoerus heseloni, Metridiochoerus compactus, Equus cf. oldowayensis, and Elephas recki (T.H., pers. obs.). Together, the fauna and lithic industry help further constrain the age of the LNB, providing a best-estimate age of ~1.7-1.2 Ma (equivalent to Olduvai Bed II; Deino et al., 2021).

2. Materials and methods

The comparative extant sample comprises 278 guenon specimens including species from all six genera (Table 1; SOM Tables S2 and S3). In addition, 35 fossil specimens representing at least three taxa (*N. browni*, cf. *Erythrocebus*, and cf. *Chlorocebus* sp. indet. from

J.L. Arenson, T. Harrison, E.J. Sargis et al. **Table 1** Sample sizes of the comparative sample: total (female/male/unknown).

Species	Cranial/ mandibular	Dental	Total
Allenopithecus	12 (5/7)	16 (7/9)	16 (7/9)
nigroviridis			
Allochrocebus	21 (12/9)	21 (12/9)	21 (12/9)
lhoesti	4 (0 (0)	1 (0 0)	4 (0 (0)
Allochrocebus	4 (2/2)	4 (2/2)	4 (2/2)
preussi	17 (7/10)	10 (0/10)	20 (0/11)
Cercopithecus albogularis	17 (7/10)	19 (9/10)	20 (9/11)
Cercopithecus	14 (6/8)	17 (8/9)	22 (9/13)
ascanius	14 (0/0)	17 (8/5)	22 (3/13)
Cercopithecus mitis	19 (6/13)	20 (7/13)	22 (8/14)
Cercopithecus	20 (9/11)	14 (7/7)	20 (9/11)
neglectus	20 (0/11)		20 (0/11)
Cercopithecus	9 (2/7)	9 (2/7)	9 (2/7)
nictitans			
Cercopithecus	3 (0/3)	3 (0/3)	3 (0/3)
pogonias			
Chlorocebus	5 (3/2)	6 (3/3)	6 (3/3)
aethiops			
Chlorocebus	9 (4/5)	12 (7/5)	12 (7/5)
cynosuros			
Chlorocebus dryas	5 (2/3)	4 (1/3)	5 (2/3)
Chlorocebus	29 (11/18)	35 (15/20)	36 (15/21)
pygerythrus			
Chlorocebus sabaeus	11 (6/5)	11 (6/5)	13 (7/6)
Chlorocebus	12 (5/7)	14 (7/7)	14 (7/7)
tantalus	42 (510)	24 (2/45)	24 (0/45)
Erythrocebus patas	13 (5/8)	24 (9/15)	24 (9/15)
Miopithecus	4 (2/2)	4 (2/2)	4 (2/2)
ogouensis Miopithecus	11 (4/7)	29 (20/9)	32 (20/12)
talapoin	11 (4/7)	29 (20/9)	32 (20/12)
cf. Chlorocebus	5 (3/2)	30 (10/5/15)	31 (10/6/15)
sp. indet.	3 (3/2)	30 (10/3/13)	31 (10/0/13)
cf. Erythrocebus sp.	2 (1/1)	1 (0/1)	2 (1/1)
indet.	2 (1/1)	1 (0/1)	2 (1/1)
Nanopithecus	1 (0/0/1)	2 (0/0/2)	2 (0/0/2)
browni	- (-1-1-)	- (-,-,-)	= (-, 3,2)
Total	226 (95/130/1)	295 (134/144/17)	318 (141/160/17)

Table 2 List of linear craniomandibular measurements and calculated indices.

Region	Measurement	Description
Cranium	Midface height	Vertical height from the inferior margin of the orbit to the maxillary alveolar margin
	Zygomatic depth	Vertical height from the inferior margin of the orbit to zygomaxillare
	Maxillary alveolar height	Zygomaxillare to lateral alveolar margin below zygomatic insertion
	Inferior rostral length	Distal margin of M ³ to prosthion
	Premaxillary length	Inferior-most point of the maxillary-premaxillary suture to prosthion
	Maxillary alveolar length	Mesial margin of C ¹ to distal margin of M ³
	Maxillary bicanine breadth	External maximum breadth of the maxilla over the maxillary canines
	Maxillary molar row length	From mesial M ¹ to distal M ³
	Maxillary postcanine length	From mesial P ³ to distal M ³
Mandible	Corpus height at M ₁	Superior-inferior height of the corpus under M ₁ taken buccally
	Corpus width at M ₁	Mediolateral breadth of the corpus at the level of M ₁
	Corpus height at M ₂	Superior-inferior height of the corpus under M ₂ taken buccally
	Corpus width at M ₂	Mediolateral breadth of the corpus at the level of M ₂
	Corpus height at M ₃	Superior-inferior height of the corpus under M ₃ taken buccally
	Corpus width at M ₃	Mediolateral breadth of the corpus at the level of M ₃
	Symphysis height	Maximum height of the symphysis from infradentale to inferior-most point of symphysis
	Symphysis depth	Maximum depth of the symphysis in the sagittal plane, taken perpendicular to length
	Mandibular bicanine breadth	External maximum breadth of the mandible over the mandibular canines
	Mandibular molar row length	From mesial M_1 to distal M_3
Indices	Face shape*	Midface height/inferior rostral length
	M ¹ crown shape*	M^1 MBL/ M^1 MD
	M ² crown shape*	M^2 MBL/ M^2 MD
	M ₁ crown shape*	$M_1 MBL/M_1 MD$
	M ₃ crown shape*	M ₃ MBL/M ₃ MD
	Relative P ³ area	Square root of P^3 area (BL \times MD)/square root of M^1 area (MBL \times MD)
	Corpus shape*	Corpus height under M ₁ /mandibular molar row length
	Symphysis shape*	SI symphysis length/AP symphysis depth

Table 3Linear measurements of the cranium, mandible, and dentition of LAET 75-3703.

Measurement	Value
Midfacial height	24.0
Zygomatic depth	17.0
Alveolar height	12.0
Inferior rostral length	44.7
Premaxillary length	11.3
Maxillary alveolar length	36.6
Maxillary bicanine breadth	30.3
Maxillary molar row length	20.0
Maxillary postcanine row length	27.5
Corpus height under M ₁	16.7
Corpus width under M ₁	6.5
Corpus height under M ₂	15.4
Corpus width under M ₂	6.9
Corpus height under M ₃	15.5
Corpus width under M ₃	6.7
Symphysis SI height	23.4
Symphysis AP depth	9.7
External mandibular bicanine breadth	18.0
Mandibular molar row length	19.5
C ¹ BL	5.9
C ¹ MD	7.2
P ³ BL	3.7
P ³ MD	3.4
P ⁴ BL	5.0
P ⁴ MD	4.3
M ¹ MBL	5.6
M ¹ DBL	5.5
$M_{-}^{1}MD$	6.5
M_{\perp}^2 MBL	6.8
M_{\perp}^{2} DBL	6.1
$M_0^2 MD$	6.7
M ³ MBL	6.2
M_{\perp}^{3} DBL	5.2
M ³ MD	6.5
C ₁ BL	7.5
C ₁ MD	5.0
P ₃ BL	9.3
P ₃ MD	3.8
P ₄ BL	_
P ₄ MD	_
M ₁ MBL	4.9
M ₁ DBL	4.9
$M_1 MD$	6.1
M ₂ MBL	_
M ₂ DBL	_
M ₂ MD	6.6
M ₃ MBL	6.0
M ₃ DBL	5.2
M ₃ MD	6.5

Abbreviations: SI = superior-inferior; AP = anteroposterior; BL = buccolingual breadth; MD = mesiodistal length; MBL = mesial buccolingual breadth; DBL = distal buccolingual breadth. See Table 2 for definitions of craniomandibular linear measurements.

Asbole and Andalee) were sampled from published measurements in the literature (Table 1; SOM Tables S2 and S3). Nineteen standard measurements on the face and mandible preserved in LAET 75-3703 were taken on the comparative sample, and standard dental metrics were taken on the upper and lower canines, premolars, and molars. Definitions of the craniomandibular measurements taken and calculated indices are presented in Table 2. Additional dental metric data for some taxa were downloaded from the PRImate Morphology Online Database (PRIMO; https://primo.nycep.org), courtesy of Eric Delson and the New York Consortium of Evolutionary Primatology (NYCEP). All 19 craniomandibular measurements and standard dental metrics on the upper and lower canines through third molars for LAET 75-3703 are presented in Table 3. Raw data on the extant sample utilized in the comparative analysis are included in SOM Tables S2 and S3, and summary statistics of all measurements are presented in SOM Tables S4 and S5

Table 4Sample sizes of *Cercopithecus* and *Chlorocebus* with no missing data included in the discriminant function analysis (DFA): total (female/male).

Species	Included in DFA	
Cercopithecus albogularis	16 (7/9)	
Cercopithecus ascanius	6 (3/3)	
Cercopithecus mitis	13 (3/10)	
Cercopithecus neglectus	13 (6/7)	
Cercopithecus nictitans	5 (0/5)	
Total Cercopithecus	53 (19/34)	
Chlorocebus aethiops	1 (1/0)	
Chlorocebus cynosuros	9 (4/5)	
Chlorocebus pygerythrus	19 (8/11)	
Chlorocebus sabaeus	1 (1/0)	
Chlorocebus tantalus	9 (4/5)	
Total Chlorocebus	39 (18/21)	
Grand total	92 (37/55)	

(craniomandibular and dental metrics, respectively, for both raw data and summary statistics).

Specimens were sampled from the following institutions: American Museum of Natural History, New York; Field Museum of Natural History, Chicago; Harvard University Museum of Comparative Zoology, Cambridge; United States National Museum of Natural History-Smithsonian Institution, Washington, D.C., USA; Powell-Cotton Museum, Birchington-on-Sea, UK; and the Royal Museum of Central Africa, Tervuren, Belgium (see SOM Tables S2 and S3 for all comparative specimens included in this study).

Statistical differences in indices among genera were assessed with one-way analyses of variance (ANOVAs), and pairwise differences were explored post hoc with Tukey's honest significant difference (HSD) multiple comparisons tests. The probability that LAET 75-3703 was sampled from a given taxon was assessed with a single-case test, which is analogous to a Student's t-test but where the variance of one sample cannot be estimated (Sokal and Rohlf, 1995). Statistical significance of the single-case tests was evaluated with a Holm-Bonferroni correction to adjust for an elevated type I error rate when conducting multiple comparisons. The reported *p* values for the single-case tests are scaled adjusted values following a Holm-Bonferroni correction.

To further explore the affinities of LAET 75-3703 with *Chlorocebus* and *Cercopithecus*, a discriminant function analysis (DFA) was performed on a subsample of 92 modern individuals comprised of 53 *Cercopithecus* and 39 *Chlorocebus* specimens with no missing data for the seven included variables (Table 4). A subsample of the guenon comparative sample was selected to avoid small sample sizes for some taxa and to reduce noise in the analysis by constraining it to likely extant candidates (see Subsection 3.2.). The analysis included seven indices of the face, dentition, and mandible that were both deemed informative in separating *Chlorocebus* and *Cercopithecus* and were preserved on LAET 75-3703 (Table 2). All analyses were performed in R v. 3.4.4 (R Core Team, 2018), using the package 'MASS' for the discriminant function analysis (Venables and Ripley, 2002) and the packages 'ggplot2' (Wickham, 2016) and 'ggpubr' (Kassambara, 2020) to generate plots.

This published work and the nomenclatural acts it contains have been registered with ZooBank: LSID, urn:lsid:zoobank.org:pub: 58E3E4ED-ED09-4149-B661-4810ADFF4D51.

3. Systematic paleontology

Order Primates Linnaeus, 1758 Infraorder Catarrhini É. Geoffroy Saint-Hilaire, 1812

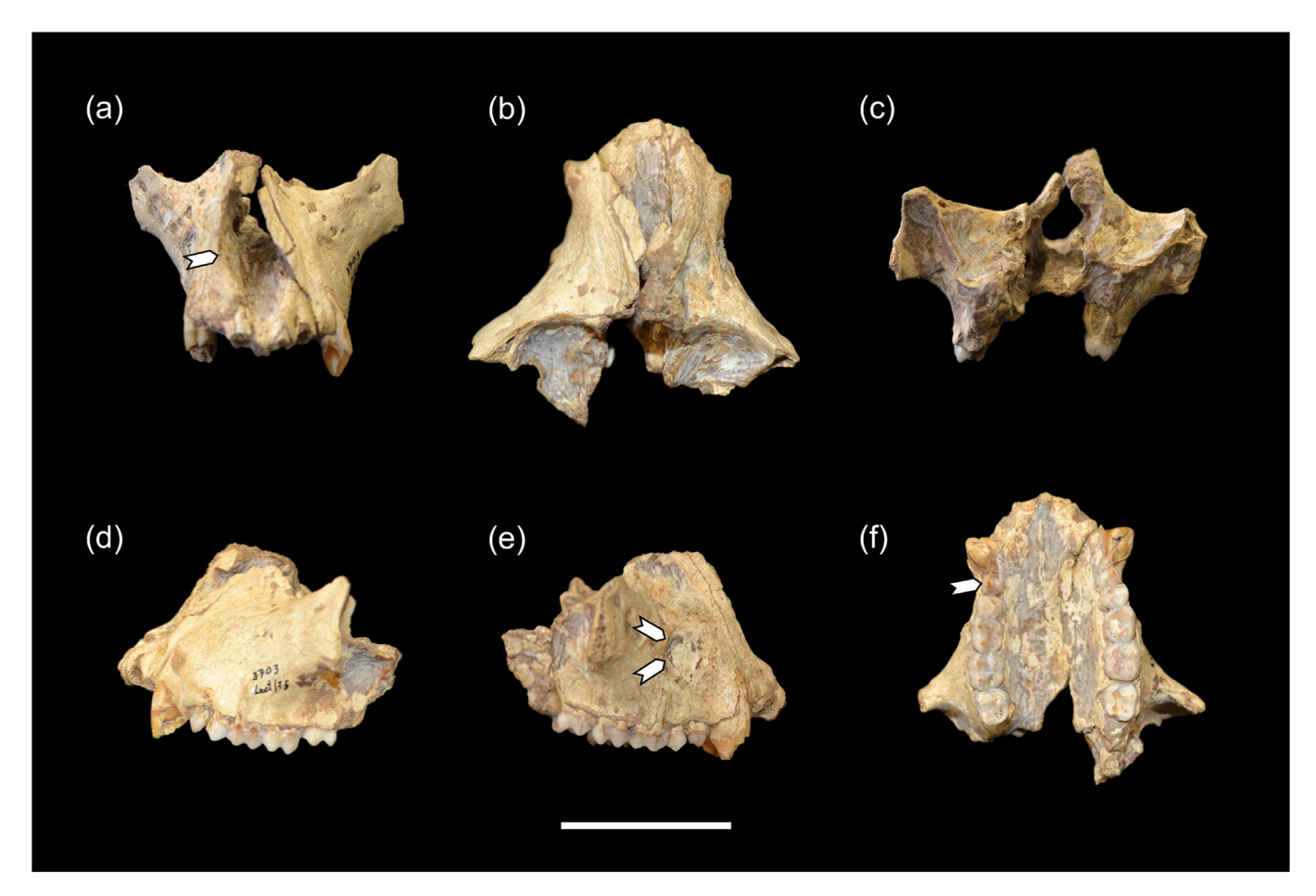


Figure 3. Views of the LAET 75-3703 cranial fragment: a) anterior; b) superior; c) posterior; d) left lateral; e) right lateral; f) inferior (palatal) views. White arrows in (a) highlight angulation of the lateral nasal aperture margin; in (e) outline the small thumbprint depression on the maxilla; and in (f) mark the very small P³. Scale bar = 3 cm.

Superfamily Cercopithecoidea Gray, 1821 Family Cercopithecidae Gray, 1821 Subfamily Cercopithecinae Gray, 1821 Tribe Cercopithecini Gray, 1821 Genus *Chlorocebus* Gray, 1870 *Chlorocebus* ngedere sp. nov. (Figs. 3 and 4)

Holotype LAET 75-3703, associated lower face and mandible. Type locality Locality 1, Lower Ngaloba Beds, Laetoli, Tanzania. Age and distribution Early Pleistocene. The beds are poorly constrained with radiometric dating, but are estimated at ~1.7—1.2 Ma in conjunction with faunal and archaeological evidence. Etymology The species name 'ngedere' is the Kiswahili name for the vervet monkey.

<u>Diagnosis</u> A relatively large cercopithecin monkey, lacking a hypoconulid on the M₃, a distinct dental feature uniting all known cercopithecins. Shares with *Chlorocebus*, and is differentiated from *Cercopithecus*, by the combination of the following features: the presence of small bounded 'thumbprint' depressions on the maxillae, a tall and narrow nasal aperture with angled lateral margins, relatively buccolingually broad molars, and a shallow mandible that decreases in depth posteriorly. Males similar in skull dimensions to large male individuals of *Chlorocebus tantalus*, *Chlorocebus pygerythrus*, and *Chlorocebus sabaeus*, but typically larger than *Chlorocebus aethiops*, *Chlorocebus cynosuros*, and

Chlorocebus dryas. Differs from Ch. tantalus and Ch. aethiops in having a buccolingually broader and less elongate M₃. Differs from most Chlorocebus specimens in preserving an unreduced distal M³ with a complete distal loph. Differs from Ch. dryas in its much larger size and in lacking adaptations for folivory/insectivory in the dentition (i.e., relatively lower molar cusps than in Ch. dryas). Differs from all known species of Chlorocebus in having a very small P³ relative to M¹. No skeletal material or published morphological data for Chlorocebus djamdjamensis were available for comparison.

3.1. Description of LAET 75-3703

LAET 75-3703 represents a partial skull consisting of the lower face and mandible. The cranial portion preserves the premaxillae and maxillae, palate, anterior zygomatics, and a fragment of the inferior portion of the nasals. The upper dentition includes the left and right I^1 roots, left and right canine crown bases, and left and right P^3-M^3 crowns (Fig. 3). The mandibular portion preserves the symphysis, a short portion of the left corpus as far as the P_4 , and the entire, but crushed, right corpus and anterior part of the ramus. The mandible preserves the roots of the left and right incisors and canines, anterior root of the left P_3 , crown of the right P_4 . The right corpus preserves a heavily worn and abraded M_1-M_2 and the nearly complete crown of M_3 , missing only the entoconid, which is broken at the base (Fig. 4).

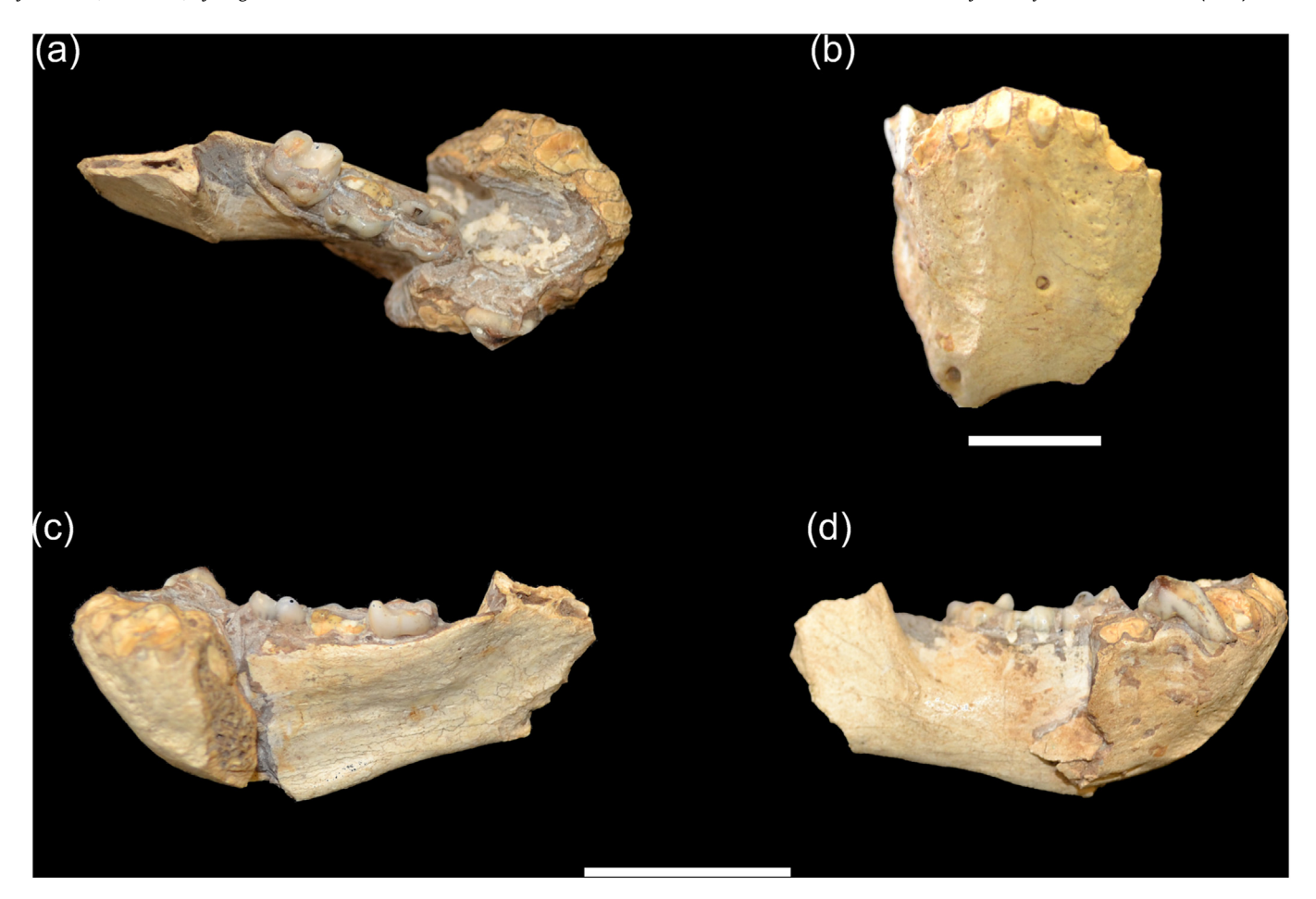


Figure 4. Views of the LAET 75-3703 mandible: a) superior; b) anterior; c) lingual; d) buccal views. The right M_1 and M_2 crowns are heavily worn and abraded occlusally, but the M_3 crown is mostly intact, although the entoconid is broken off. It lacks a hypoconulid on M_3 and has a median mental foramen and well-marked mental ridges on the symphysis and a shallow mandible that is deeper anteriorly. Scale bar for (a, c-d) = 2 cm; scale bar for (b) = 1 cm.

Cranium The cranial fragment consists of the lower face, rostrum, and palate, including the anterior zygomata and the inferior margin of the left and right orbits to approximately the vertical plane distal to M³, but slightly farther posteriorly on the left side (Fig. 3). Facial sutures are visible, including the zygomaticomaxillary, maxillarypremaxillary, and nasomaxillary sutures. Small fragments of the lacrimal bones are present, and the nasolacrimal sutures are visible along the inferior margin of the orbits on both sides. The palate preserves the left and right C¹ through M³, but both canines are broken near the base. The external bone of the maxilla covering the canine juga is weathered, and the bases of both canine roots are partially exposed. All four incisor crowns are missing, but the left and right I¹ roots are visible. The I² alveoli are filled with sediment, indicating that both upper lateral incisors were lost before fossilization. The molars and premolars are well preserved with moderate to heavy wear. The lingual cusps on the molars are worn so that broad dentine lakes are exposed. These are connected mesiodistally by a narrow strip of dentine exposure on M¹ and M². Point wear is present on the buccal cusps with variable levels of wear buccolingually along the lophs (corresponding to wear grades D–E along the molar row; Delson, 1973).

The specimen is deformed along the midline such that the left and right sides are not evenly aligned, and the right side is displaced superiorly relative to the left side. The superior left maxilla is deformed toward the right, and the left inferior orbital margin appears artificially mediolaterally elongated compared with the

right. Most of the foramina and cracks are filled with reddishbrown fine-grained cemented sediment. The floor of the nasal cavity is also filled with sediment obscuring the incisive foramen. There is no evidence of insect damage, root markings, or gnaw marks from rodents.

The rostrum of LAET 75-3703 is of moderate length and relatively narrow with low subnasal prognathism. The anteroposterior length of the rostrum from the premaxilla to the anterior margin of the orbit is 33.8 mm. In superior view, the snout is rectangular with a convex premaxilla that projects anteriorly beyond the canine juga. The premaxilla is relatively narrow with a maximum mesiodistal width inferiorly of 20.1 mm. In the midline, the subnasal region of the premaxilla is shallow with a minimum dorsoventral height of 6.4 mm. The premaxillae extend superiorly past the inferior margin of the orbits, but they are broken before their superior limit. Nevertheless, it is clear from their configuration that they would have made contact with the nasals and excluded the maxilla from bordering the nasal aperture. The minimum mediolateral breadth (2.8 mm) of the premaxilla occurs at the level of the widest diameter of the nasal aperture. A small piece of the right nasal bone is preserved floating on attached sediment, not in articulation with the premaxilla, and is too fragmentary to determine the original shape or extent of the nasals. Although the specimen is distorted along the midline, the shape of the nasal aperture would have been tall and narrow, forming a slight diamond shape with the greatest breadth of the aperture at midheight (Fig. 3a). The nasal aperture tapers inferiorly between the laterally splayed roots of the central incisors. Viewed posteriorly, the nasal cavity preserves the posterior portion of the right maxilloturbinate (Fig. 3c).

The low canine juga are oriented mediosuperiorly and border the lateral aspect of the nasal aperture. There are shallow, small thumbprint-like round depressions on the maxillae, delimited by raised superior and posterior margins, just anterior to the infraorbital foramina above P³ and P⁴ (Fig. 3e). There are six infraorbital foramina on the left and five on the right positioned just below the inferior plane of the orbit. Two left and one right zygomaticofacial foramina are visible just above the inferior plane of the orbit. A tiny subsidiary foramen is present on the left and right sides just inferior to the main foramina. A shallow secondary elliptical fossa is located on the maxilla between the infraorbital foramina and the zygomaticofacial foramina.

The zygomatic process inserts above the M^2/M^3 contact and is angled superiorly at approximately 130° relative to the lateral face of the maxilla. The zygomatic process originates 9.4 mm above the plane of the alveolar margin. The maxillary process of the zygomatic is shallow (the length of the zygomaticomaxillary suture is 16.4 mm) relative to the inferosuperior height of the lower face (25.2 mm from the alveolar margin at M^2 to the inferior border of the orbit), although the midface is shallow overall. The anterior root of the zygomatic arch is preserved on the left side and shows that it was relatively slender in the inferosuperior plane.

The inferior orbital margin is distorted and artificially elongated on the right side but appears to preserve the original contour on the left. The orbital margin is sharp and elevated well above the orbital floor. The inferior margin of the orbit is positioned vertically above the mesial moiety of M² just anterior to the root of the zygomatic process. Unfortunately, not enough of the orbit is preserved to determine the size and shape. The orbital process of the zygomatic forming the lateral orbital rim is partially preserved on the left side. It is relatively narrow with a sharp lateral margin separating the facial aspect of the zygoma from the temporal fossa. The zygomaticomaxillary suture can be traced posteriorly onto the postorbital wall and ends at a shallow depression, partially obscured by a thin layer of sediment and bordered posteriorly by a shallow vertical ridge. The latter represents the inferior junction of the sphenoid bordering a small inferior orbital fissure.

The palate is relatively long and narrow with gently outwardly bowed lateral sides. The posterior margin is incomplete, so it is not possible to obtain a precise measurement of the palate length, but it can be estimated to have been ~46 mm. The maximum mediolateral breadth of the palate occurs at M² (the internal breadth is

18.6 mm, and the external breadth is 32.6 mm). In palatal view, the narrow premaxilla protrudes anteriorly well beyond the level of the canines. The incisor roots and alveoli are arranged in an arc, with the lateral incisors being more posteriorly placed than the central incisors. A short diastema (3.8 mm) separates the alveolus of the I² from the canine. Posterior to the central incisors is a prominent sagittal ridge, the nasal crest, which subdivides the large oval incisive fenestra. The palate is relatively shallow anteriorly but deepens posteriorly with steep-sided alveolar processes in the region of the cheek teeth. An irregular intermaxillary suture is discernible in the midline of the palate, but there is no evidence of a palatine-maxillary suture or a greater palatine foramen.

Upper Dentition The incisor crowns are missing, and only the central incisor roots are preserved. The broken cross sections of the roots of the I¹s are oval, being labiolingually broader (5.0 mm) than they are mesiodistally long (3.6 mm). The alveoli for the I^2 s are also oval and are somewhat smaller (4.6 \times 3.1 mm) than those of the central incisors. Although the canines are broken near the base, the crowns are robust, markedly bilaterally compressed, and exhibit a mesial sulcus that extends onto the root. The size of the canines in relation to the other teeth indicates that the specimen is most likely a male individual. The P³ is very small, with a vestigial protocone represented by a low and indistinct swelling on the lingual cingulum. The paracone is tall with well developed and sharp mesial and distal crests, and a low, rounded, and obliquely oriented transverse crest links the two cusps. There is a small fissure-like mesial fovea and a much larger triangular distal fovea. P⁴ is much larger than P³, and it is bicuspid, with a low rounded protocone and a much taller paracone. The paracone is slightly mesially inclined with a longer distal than mesial crest. A low and rounded transverse crest connects the two cusps. The mesial fovea is represented by a narrow fissure, and the distal fovea forms a relatively short crescent-shaped basin distal to the transverse crest. There are no mesial or distal accessory cusps.

The maxillary postcanine tooth rows exhibit a slight lateral bowing with M^2 placed more laterally than the M^1 and M^3 . In addition, the buccal margin of M^3 tapers distally, accentuating the curvature of the maxillary tooth row. The molars are bilophodont and slightly longer than broad. Molar flare is low with the cusp tips placed toward the periphery of the crown. Overall, the crown height is low, with low cusps and a shallow median buccal notch. The paracone and metacone have short, sharp crests running mesially and distally from the apices. The protocone and hypocone are worn with small areas of dentine exposure, and the paraloph and metaloph are partially worn but appear to have been relatively

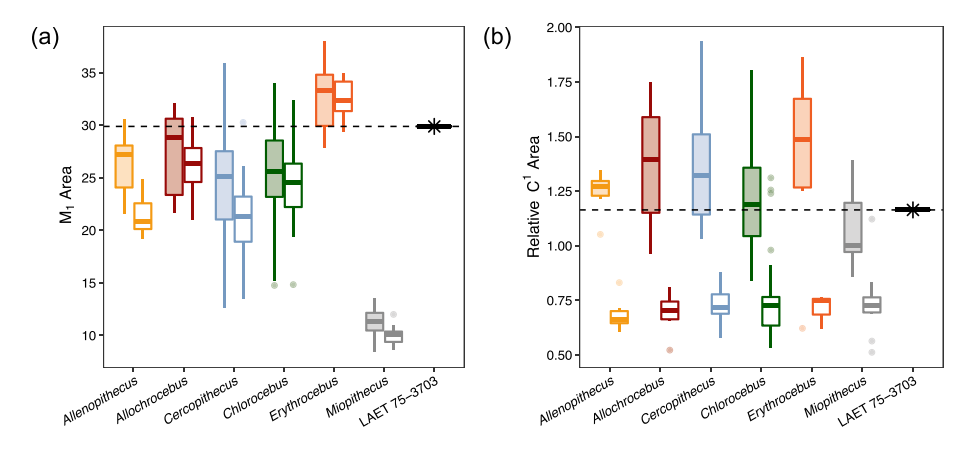


Figure 5. Boxplots showing dental proxies of size and sex. For both, filled boxes represent the distribution of males and unfilled boxes represent females: a) M_1 area as a proxy for body size among guenons; b) relative canine size across guenons (calculated as upper canine base area/ M^1 area).

low and rounded surrounding a shallow central basin. The mesial shelf is slightly longer than the distal shelf. The molar size order is $\mathsf{M}^1 \approx \mathsf{M}^3 {<} \mathsf{M}^2.$ On M^1 and $\mathsf{M}^2,$ the distal cusps are slightly smaller than the mesial cusps, and the crowns narrow slightly distally. The crown of M^3 tapers even more strongly distally, especially on the lingual side. The two distal cusps on M^3 are small and closely associated, rather than twinned or appressed, with a distinct metaloph and a distal fovea that is reduced to a small dimple on the distal margin of the crown. The roots of the postcanine teeth are exposed at the buccal alveolar margin and appear to bifurcate close to the cementum-enamel junction. All of the upper premolars and molars have three roots.

<u>Mandible</u> The mandibular symphysis and the right corpus are preserved with P_3 and M_1 – M_3 (Fig. 4). The crowns of M_1 and M_2 are heavily worn, and M_3 is moderately worn. The roots of all four incisors and both canines are visible in cross section in the symphysis, and the roots of the right P_4 and the mesial root of the left P_3 are also preserved. On the right side, the corpus is broken distal to P_4 and displaced medially. The corpus extends posteriorly past M_3 , preserving the inferior portion of the oblique line and a short section of the ramus. The ramus is broken just superior to the level of the molar

occlusal plane. The incisal region of the symphysis is narrow. The incisor roots are arranged in an arc, with the lateral incisors positioned more posteriorly than the central incisors. Anteriorly, the symphyseal region slopes posteriorly at approximately 60° relative to the alveolar plane in a gentle curve from the incisor alveolar margin to the inferior torus (i.e., the simian shelf). In the midline region of the anterior face of the symphysis is a relatively smooth triangular area that is narrow superiorly below the central incisors and broadens inferiorly. This area is bordered bilaterally by welldeveloped mental ridges that form low irregular crests and extend laterally onto the inferior aspect of the corpus. A small median mental foramen is present on the midline of the symphyseal face inside the smooth triangular area. The internal surface of the symphysis has a short sloping alveolar planum, a shallow genioglossal fossa, and a slender inferior torus that extends posteriorly to vertically below P₄. Laterally, the external face of the corpus has weakly developed canine juga and a small shallow circular depression or fossa just below P₃. On the lateral aspect of the corpus, vertically below the mesial root of P₄ and located close to the inferior border, is a large elliptical mental foramen and a pair of tiny subsidiary foramina just superior to the primary foramen. The corpus shallows

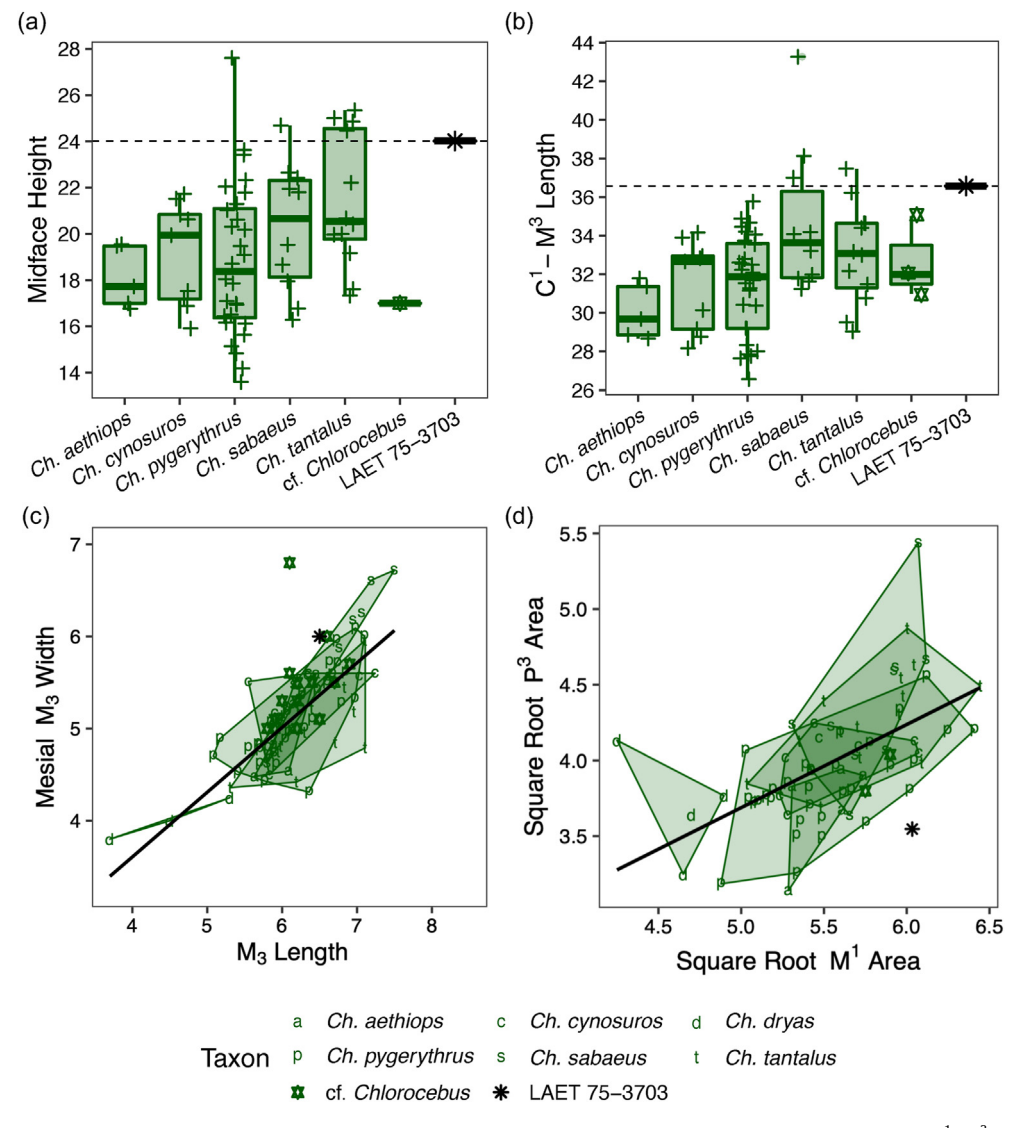


Figure 6. Comparison of LAET 75-3703 craniodental metrics with extant and fossil *Chlorocebus*: a) midfacial height; b) dental size, measured as C^1 – M^3 length; c) M_3 shape plotted as mesial buccolingual breadth against mesiodistal length; d) square root of P^3 area against the square root of M^1 area. Data on cf. *Chlorocebus* include material from Asbole and Andalee (see text). See also Figure 11 and SOM Figure S2.

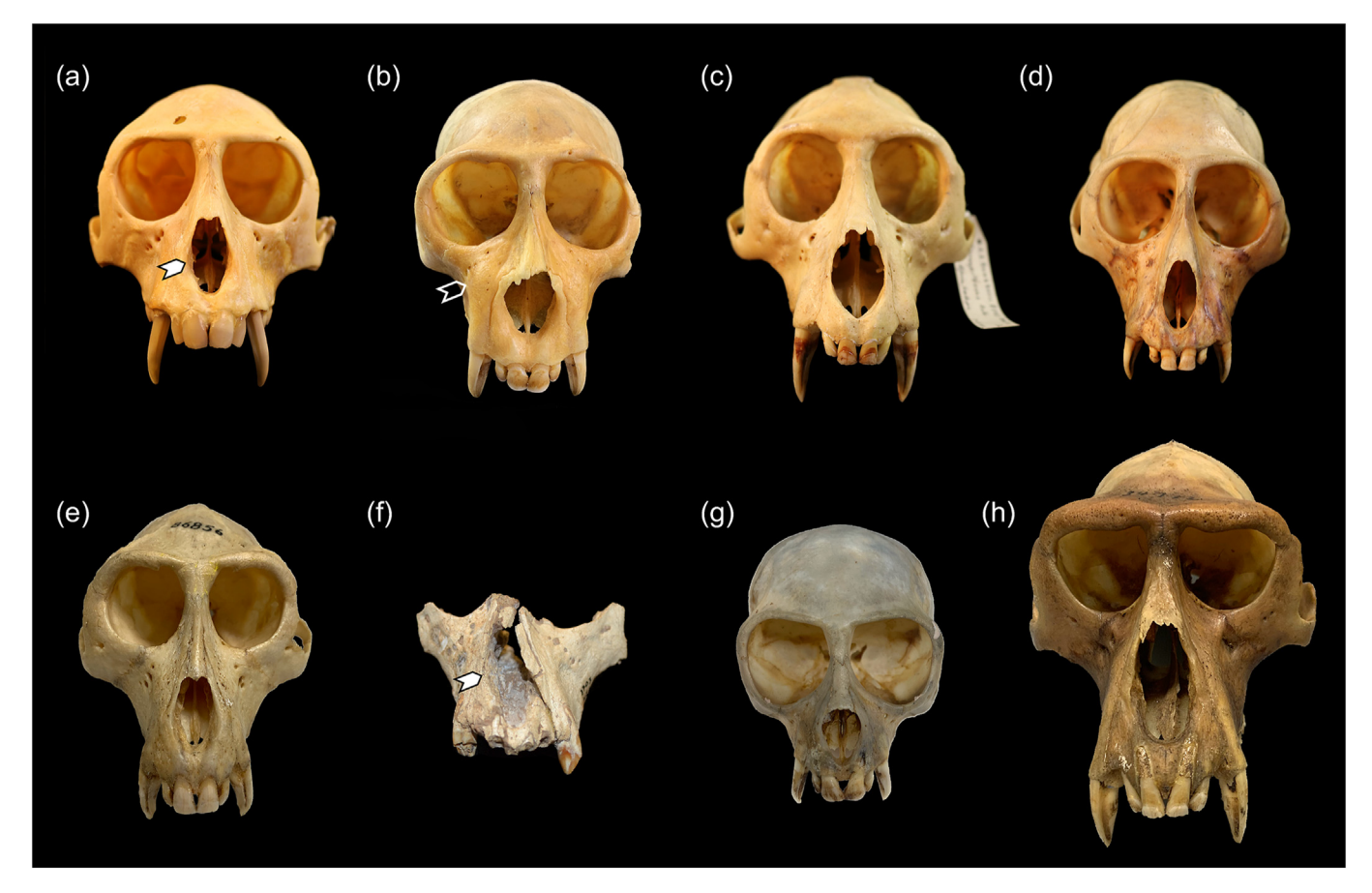


Figure 7. Male guenon crania and LAET 75-3703 in anterior view: a) *Chlorocebus pygerythrus* (MCZ 62931); b) *Allochrocebus lhoesti* (MCZ 39386); c) *Cercopithecus mitis* (MCZ 8303); d) *Cercopithecus neglectus* (MCZ 31740); e) *Allenopithecus nigroviridis* (AMNH M–86856); f) LAET 75-3703 cranial fragment; g) *Miopithecus ogouensis* (AMNH M–119638); h) *Erythrocebus* (a, MNH M–34712). Specimens are scaled to approximately equal I¹ width and are not to scale. Note the angulation of the lateral margin of the nasal aperture in *Chlorocebus* (a, white arrow) but the short, rounded nasal aperture in *Allochrocebus* (b) and the rounded margins in *Cercopithecus* (c–d). LAET 75-3703 also lacks the maxillary ridges in *Allochrocebus* (b, open arrow) and the allometrically mediated distinctive morphologies of the diminutive *Miopithecus* (g) and large *Erythrocebus* (h).

posteriorly with a minimum depth below M_3 . Laterally, the oblique line originates below mid-corpus at a rugose tubercle, vertically in line with the distal margin of M_3 , and then passes superiorly to form the sharp anterior margin of the ramus. The base of the anterior margin of the ramus slopes posteriorly approximately 120° relative to the alveolar plane of the lower molars. The ramus would not have overlapped the molar series in lateral view, leaving a substantial retromolar gap, but the extramolar sulcus is relatively narrow. The inferior margin of the corpus is relatively slender with a slightly thickened buttress on the internal surface. On the internal surface of the corpus, a fine mylohyoid line originates just posterior to M_3 and passes obliquely below the molars.

Lower dentition The lower dentition is not as well preserved as the upper dentition. The broken cross sections of the incisor roots are bilaterally compressed, and the lateral incisor roots are slightly smaller than those of the central incisors. The canine roots are oval in cross section with a shallow mesial sulcus. The right P_3 crown preserves the mesial flange, which exhibits a long canine wear facet with exposed dentine, again suggesting the specimen is probably male. The protoconid has a long mesial crest that ends in a small protostylid. Mesially, there is a slight trace of a lingual cingulum. The distal and distolingual crests delimit a narrow distal basin. The P_4 crowns are missing, but the roots are preserved and show the mesial and distal roots are fused at their base. M_1 preserves the lingual cusps and the buccal enamel wall, but the buccal half of the crown has a large area of dentine exposure. The lingual cusps of M_2 have

been lost through abrasion, and the buccal side of the crown has a large area of dentine exposure. The crowns of M_1 and M_2 are longer than broad with a slight mesial tapering. The size order of the lower molars is $M_1 < M_2 < M_3$. Owing to the wear and damage on M_1 and M_2 , it is not possible to discern details of their occlusal morphology. M_3 is better preserved, but the tip of the entoconid is missing, the protoconid is worn and abraded, and the hypoconid is worn. The crown tapers distally. The metaconid, the only intact cusp, is relatively tall and conical with relatively sharp and steeply inclined mesial and distal crests. The metalophid is low and rounded. The mesial shelf is broad, and the central basin is relatively expansive. The entoconid and hypoconid are smaller than the mesial cusps and positioned closely together. There is no hypoconulid.

3.2. Comparisons

<u>Cranium</u> Dentally, LAET 75-3703 is large for a guenon and plots above the mean values of males of most genera except for *Erythrocebus* using M_1 area as a proxy for size (Fig. 5a). Among *Chlorocebus*, it is most similar in size to large males of *Ch. sabaeus*, *Ch. tantalus*, *Ch. pygerythrus*, and cf. *Chlorocebus* from Andalee and larger than *Ch. aethiops*, *Ch. cynosuros*, *Ch. dryas*, and cf. *Chlorocebus* from Asbole in most metrics (Fig. 6; SOM Table S2). Compared with *Chlorocebus* taxa for which comparative data were available, LAET 75-3703 is significantly larger in midfacial height (single-case test LAET 75-3703 vs. all species, p < 0.05) and in dental size except for

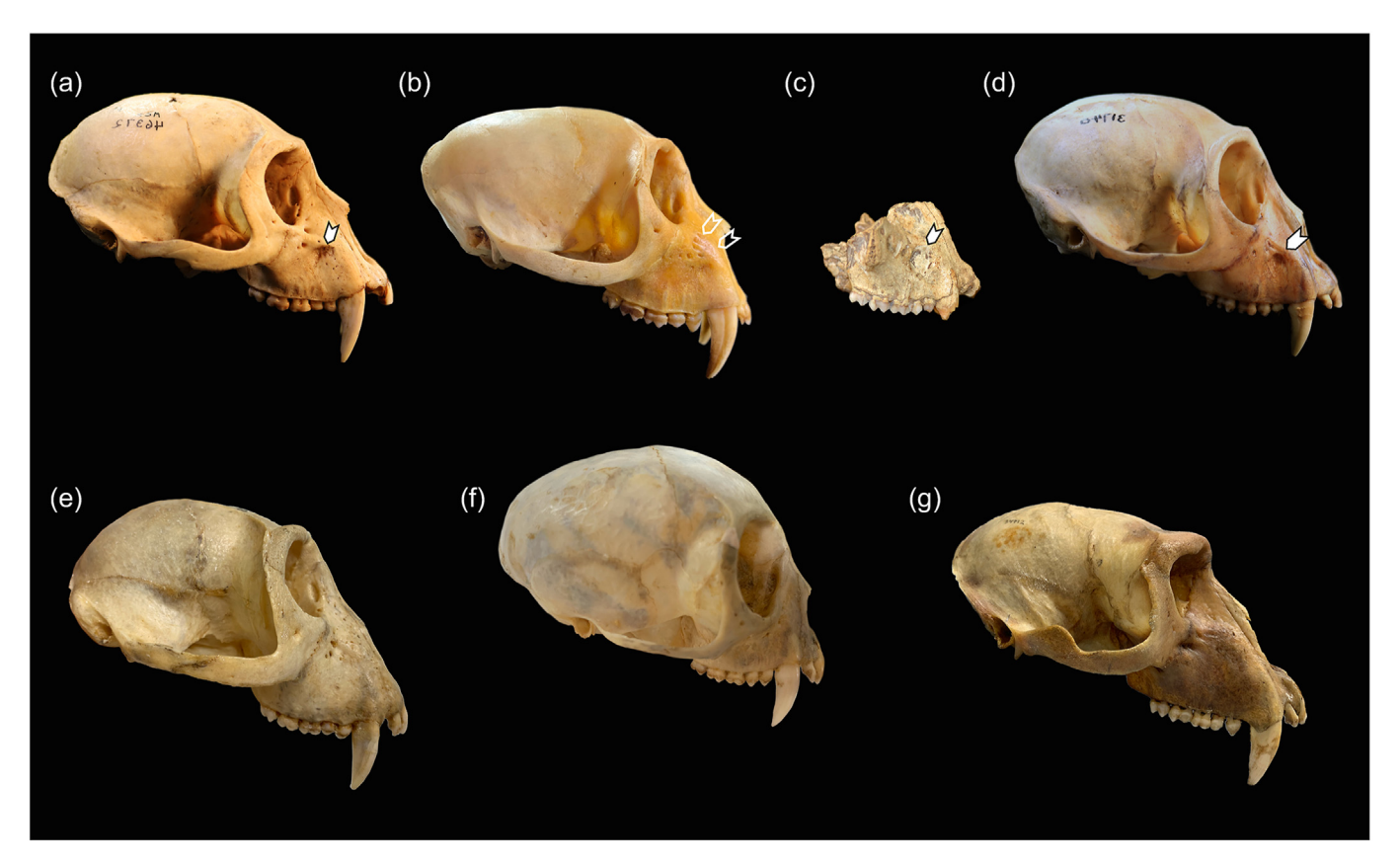


Figure 8. Male guenon crania and LAET 75-3703 in lateral view: a) Chlorocebus sabaeus (reversed; MCZ 46372); b) Allochrocebus lhoesti (MCZ 39386); c) LAET 75-3703 cranial fragment; d) Cercopithecus neglectus (reversed; MCZ 31740); e) Allenopithecus nigroviridis (AMNH M—86856); f) Miopithecus ogouensis (reversed; AMNH M—119638); g) Erythrocebus patas (AMNH M—34712). Specimens are aligned on the Frankfurt horizontal and scaled to approximately equal prosthion-inion length and not to scale. White arrows on Chlorocebus (a), LAET 75-3703 (c), and Ce. neglectus (d) highlight small maxillary depressions, clearly bounded superiorly in Chlorocebus and LAET 75-3703 and slightly broader and more diffuse in Ce. neglectus. Open arrows on Allochrocebus (b) outline the maxillary ridge, superior to a broad and shallow maxillary fossa.

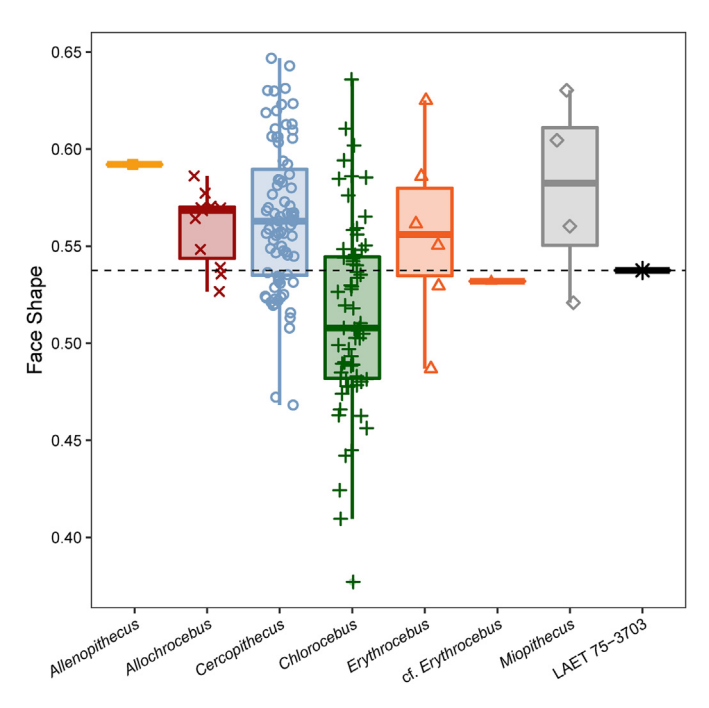


Figure 9. Boxplot showing the distribution of face shape calculated as midface height divided by inferior rostral length (see Table 2 for definition of linear measurements and SOM Table S2 for raw data). See also SOM Figure S1.

Ch. sabaeus and cf. Chlorocebus from Asbole (C^1 – M^3 length; singlecase test LAET 75-3703 vs. Ch. sabaeus and cf. Chlorocebus, p=0.21, vs. all other species, p<0.05). The relatively large upper canine (Fig. 5b) with a compressed mesial sulcus that extends onto the root and a mesially elongated honing facet on P_3 indicate that LAET 75-3703 is a male (Figs. 3 and 4). Although the canines of female guenons often resemble those of males, males can be differentiated from females by their larger canine base areas (Frost, 2001). The upper canines are broken, but the base of the tooth is preserved; estimates of the area can be made, and the relative upper canine area falls almost exclusively within the range of male guenons of similar size (Fig. 5b). Breakage or wear may make the canine base area artificially smaller, but even if it is underestimated, the canine is larger than nearly any sampled female specimen, supporting its identification as a male.

Guenons are skeletally similar, and most variation in cranial shape among guenons can be explained as a result of scaling (Cardini and Elton, 2008). LAET 75-3703 is comparable in size with larger male *Chlorocebus*, *Cercopithecus*, and *Allochrocebus* (Figs. 5 and 6), and as such, it exhibits facial morphology consistent with a guenon of that size and overlaps with both genera in nearly all linear metrics of the face and mandible (SOM Table S2). It is substantially larger than any sampled *Miopithecus* or *Nanopithecus* individual and smaller than *Erythrocebus* males. It also lacks the facial morphology associated with either of those extreme body sizes, including the abbreviated rostrum of *Miopithecus* or the boxy, elongated rostrum of *Erythrocebus* (Figs. 7 and 8). The overall shape

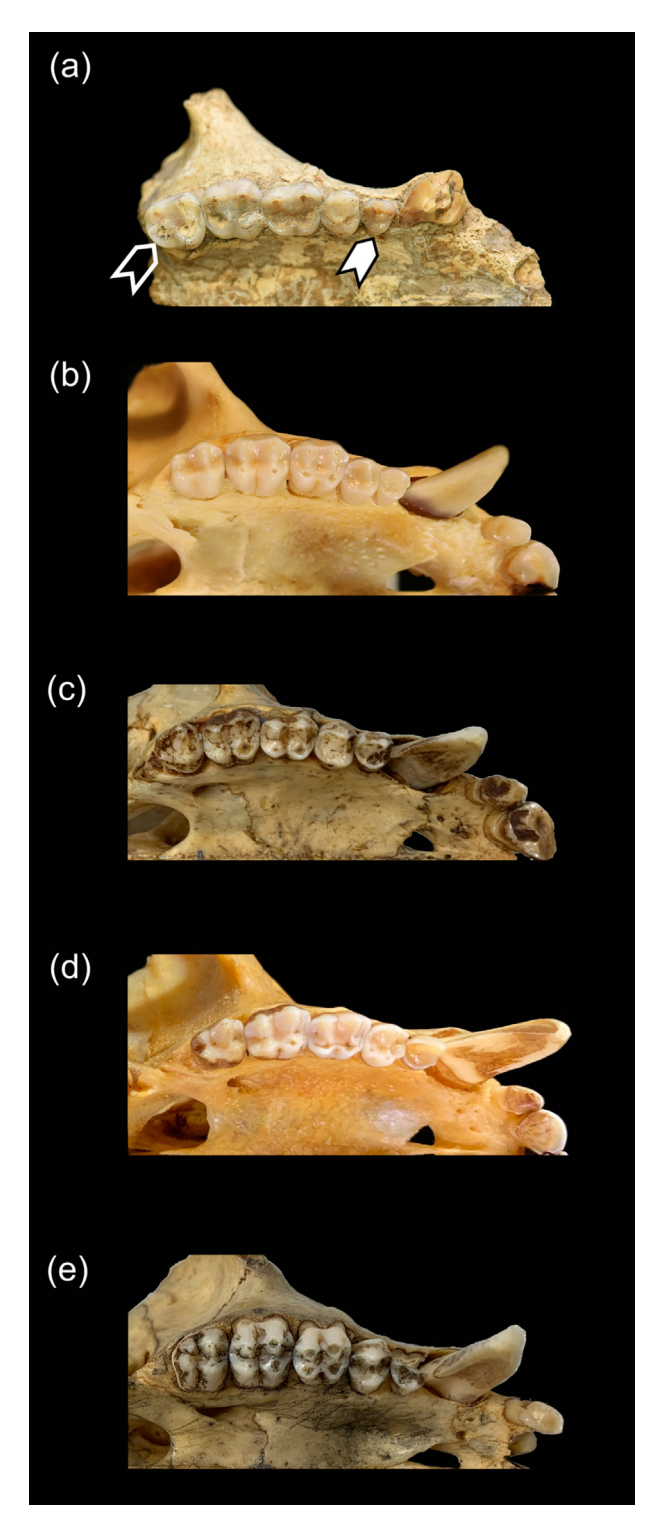


Figure 10. Guenon right palate and maxillary teeth in occlusal view: a) LAET 75-3703 cranial fragment; b) *Chlorocebus pygerythrus* (MCZ 62931); c) *Cercopithecus mitis* (AMNH M–52373); d) *Allochrocebus lhoesti* (MCZ 39386); e) *Allenopithecus nigroviridis* (AMNH M–86856). LAET 75-3703 has an extremely small P³ (white arrow) and comparatively unreduced distal M³ (open arrow).

of the face is most similar to that of larger species of *Cercopithecus* and *Chlorocebus*, especially in profile, exhibiting a rostrum of intermediate length, projecting premaxillae forming distinct subnasal prognathism, and nasal bones peaked above the maxillae (Fig. 8). *Miopithecus* and *Allenopithecus* typically have a more

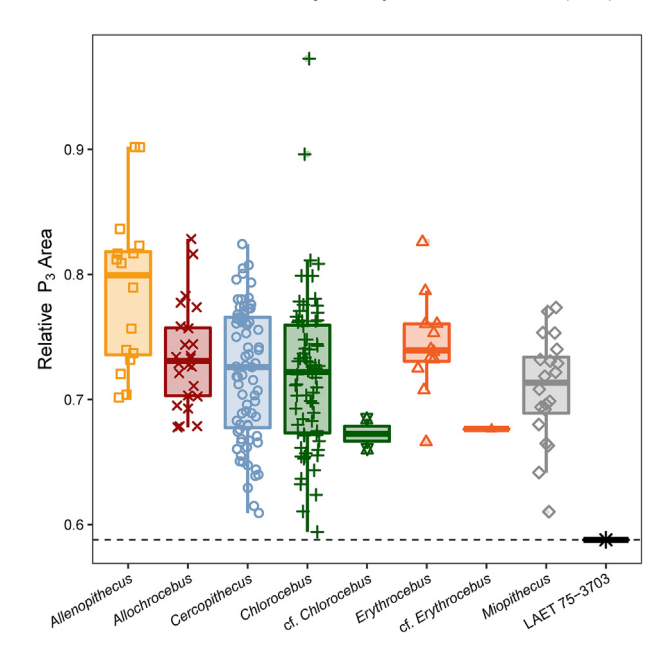


Figure 11. Boxplot showing the distribution of relative P^3 size, calculated as the square root of P^3 area divided by the square root of M^1 area. See also SOM Figure S2 to visualize the index as a scatterplot.

dorsally flattened rostrum without peaked nasals, and *Allochrocebus* has a fairly abbreviated rostrum with no subnasal prognathism. In a boxplot of face shape, measured as midface height relative to inferior rostral length, *Chlorocebus* species have a relatively elongated lower face and/or shallower midface than *Cercopithecus* and other guenon genera (ANOVA p < 0.001; Tukey's HSD *Chlorocebus* vs. *Cercopithecus*, *Allochrocebus*, and *Miopithecus*, p < 0.05; Fig. 9; SOM Fig. S1; refer also to the study by Cardini and Elton, 2008). *Erythrocebus* and *Miopithecus* are similar in this index despite their different facial morphologies because of the relative depth of the face: *Miopithecus* has a short and shallow face, whereas *Erythrocebus* has a long but superoinferiorly deeper face (SOM Fig. S1). In this regard, LAET 75-3703 falls within the distribution for both *Cercopithecus* and *Chlorocebus*, although it is below the means of all genera except *Chlorocebus*.

Several other guenon genera are also distinguishable by a suite of features. *Allenopithecus* retains primitive papionin-like features in the dentition, including marked basal flare of the molars, a relatively large P³ with a large protocone, and a less distally reduced M³ (Fig. 10e; Verheyen, 1962; Szalay and Delson, 1979). *Allochrocebus* exhibits unique facial morphology, including a relatively short rostrum, broad nasal aperture, and the presence of maxillary ridges and associated fossae in males (Figs. 7b and 8b; Szalay and Delson, 1979; Frost, 2001). As LAET 75-3703 lacks these distinctive features and shows greatest resemblance to *Chlorocebus* and *Cercopithecus*, the following comparison will primarily focus on features that distinguish the latter two genera.

Some features previously considered to be informative for separating *Cercopithecus* and *Chlorocebus*, including orbit shape (Groves, 2000; Ravi, 2013; Gilbert et al., 2021) and relative upper incisor sizes (Frost, 2001; Frost and Alemseged, 2007; Gilbert et al., 2021), are unfortunately not preserved in LAET 75-3703. However, other features in the maxilla and dentition suggest that its closest affinity is with *Chlorocebus*. On the maxilla, LAET 75-3703 exhibits small shallow 'thumbprint' depressions on the maxilla with a distinct ridge superiorly (Figs. 3 and 8). These depressions differ from the expanded maxillary fossae and pronounced maxillary

ridges seen in *Allochrocebus* males (Figs. 7 and 8; Frost, 2001). A similar depression is present in both males and females of most *Chlorocebus* specimens, especially *Ch. pygerythrus*, and is typically absent in *Cercopithecus*. Some *Cercopithecus neglectus* males exhibit shallow maxillary fossae, in some cases appearing similar to the bounded thumbprint depressions in *Chlorocebus*, but these are more often broader and shallower depressions lacking raised margins. Similar depressions have not been observed in specimens of *Erythrocebus*, *Miopithecus*, or *Allenopithecus*.

The nasal aperture of LAET 75-3703 is tall and narrow, as in species of *Chlorocebus* and many species of *Cercopithecus*, and in contrast to the short, broad, and more ovoid aperture in *Allochrocebus* (Fig. 7). In addition, *Chlorocebus* has a more angular diamond-shaped aperture than the oval or straight-sided aperture in most *Cercopithecus* species (Groves, 2000). The lateral margin of the nasal aperture of LAET 75-3703, although slightly distorted on the right side and damaged on the left side, shows a slight angle, suggesting a diamond-shaped nasal aperture as in *Chlorocebus* (Figs. 3a and 7).

<u>Upper dentition</u> As with their cranial morphology, cercopithecins are dentally similar and difficult to distinguish metrically. In particular, *Chlorocebus* and *Cercopithecus* teeth are qualitatively very similar (Eck and Howell, 1972; Delson, 1973; Szalay and Delson, 1979; Harrison and Harris, 1996). However, a few traits show separation among the cercopithecins. Overall, the dentition of LAET 75-3703 is simple and characterized by fairly low crowns and rounded cusps, lacks adaptations for folivory/insectivory as in

Allochrocebus species and Ch. dryas (Gilbert et al., 2021), and is similar to other Chlorocebus species. The premolars of LAET 75-3703 are typically cercopithecin with a relatively small P³ with variably developed protocone and much larger bicuspid P⁴ (Figs. 3 and 10). Only Allenopithecus exhibits a relatively unreduced third premolar with a well-developed protocone (P³ area relative to M¹ area. ANOVA p < 0.001: Tukev's HSD Allenopithecus vs. Miopithecus. Allochrocebus, Cercopithecus, and Chlorocebus p < 0.05), However, LAET 75-3703 is unique compared with other cercopithecins in having an especially small P3 with a narrow lingual cingulum in place of a protocone (Fig. 11; SOM Fig. S2). Within *Chlorocebus*, LAET 75-3703 has a significantly smaller P³ relative to M¹ area than all sampled species (single-case test, p < 0.05 for all species). The P⁴ is also small but not as reduced as the P³, and it exhibits a fully developed protocone. The distal shelf of P⁴ is slightly expanded and longer than the mesial shelf, but it lacks the accessory mesial and distal cuspules commonly seen in Allochrocebus (Fig. 10). A hypocone on P⁴ is occasionally observed in some *Chlorocebus* individuals as well, but they lack the proliferation of accessory cusps often seen in Allochrocebus.

The molars of LAET 75-3703 have shallow median lingual notches and low cusps. Comparative studies of cercopithecid dental morphology have previously noted that cercopithecin molars are relatively elongated compared with those of papionins (e.g., Lampel, 1963; Eck and Howell, 1972; Delson, 1973; Szalay and Delson, 1979). This is due in part to the lack of basal flare, making the teeth relatively narrower. Plots of upper and lower molar crown

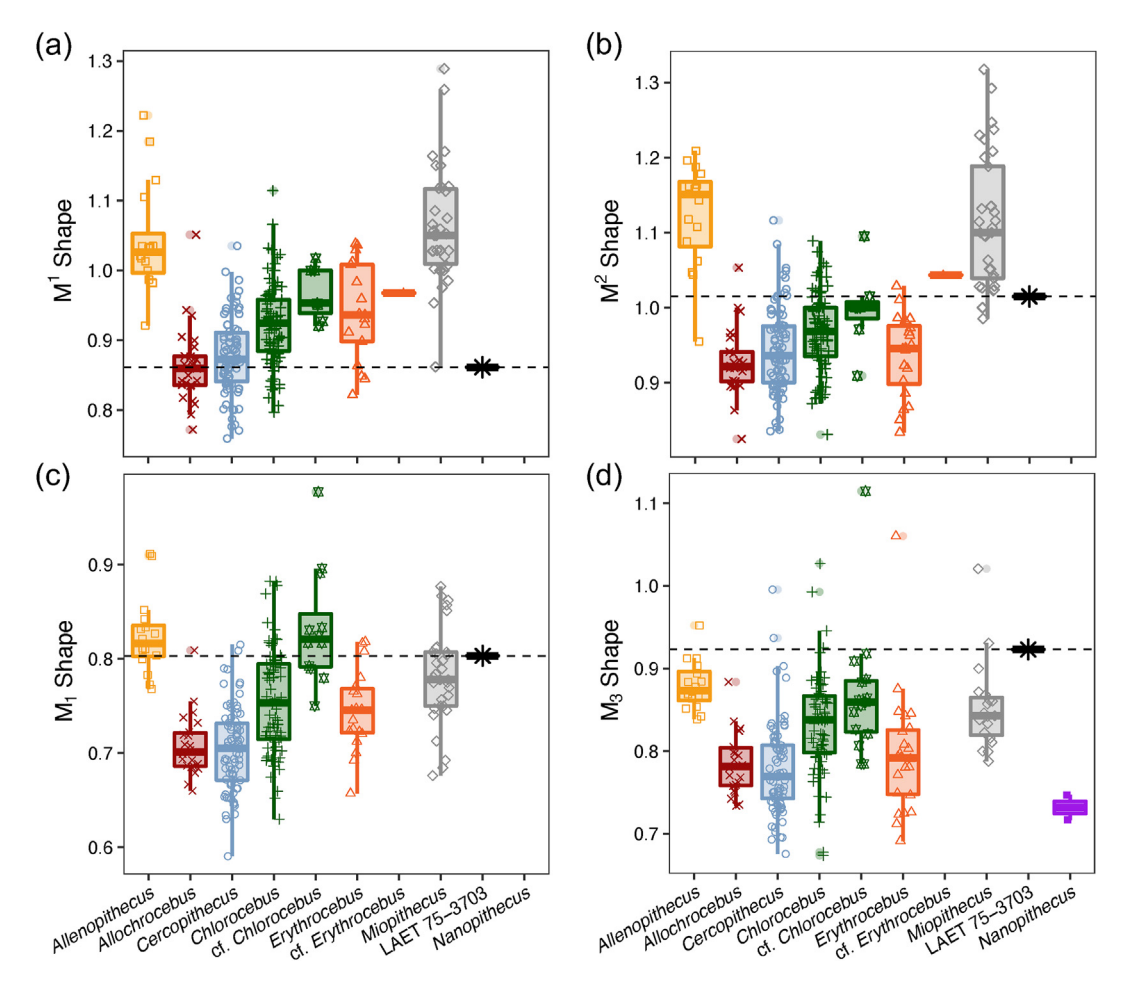


Figure 12. Boxplots of molar crown shapes calculated as the mesial buccolingual breadth divided by maximum mesiodistal length: a) M^1 crown shape; b) M^2 crown shape; c) M_1 crown shape; d) M_2 crown shape. The M^3 was excluded because it is often distally reduced, and the M_2 was excluded because it is damaged in LAET 75-3703.

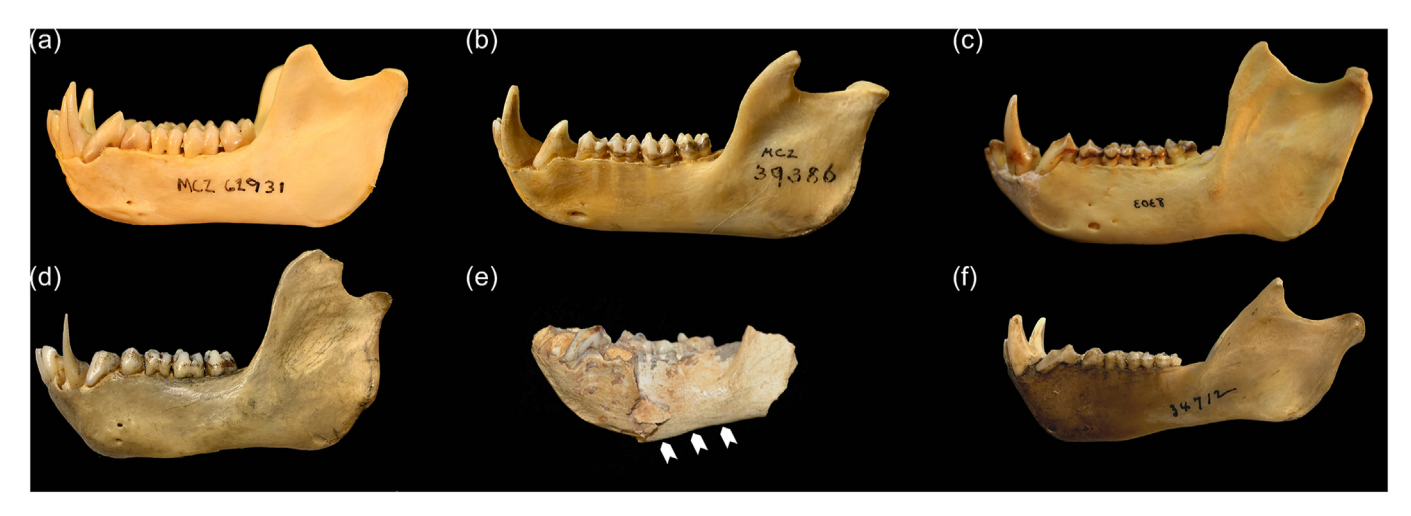


Figure 13. Male guenon mandibles and LAET 75-3703 in lateral view: a) *Chlorocebus pygerythrus* (MCZ 62931); b) *Allochrocebus lhoesti* (MCZ 39386); c) *Cercopithecus mitis* (MCZ 8303; reversed); d) *Allenopithecus nigroviridis* (AMNH M–52467); e) LAET 75-3703; f) *Erythrocebus patas* (AMNH M–34712). White arrows in (e) indicate the shallowing corpus of LAET 75-3703 posterior to the break.

shape (calculated as mesial buccolingual breadth divided by maximum mesiodistal length) show *Allenopithecus*, with its high degree of basal flare, having the broadest molars (ANOVA p < 0.05 for all molars; Tukey's HSD *Allenopithecus* vs. all genera except *Miopithecus* p < 0.05 in M_1^1 , M_2^2 , and M_3 , and vs. all genera p < 0.05 in M_1^1 ; Fig. 12). *Miopithecus* also has relatively broad molars, particularly in the maxilla, although it lacks basal flare. Molar crown shape distinguishes *Cercopithecus* and *Chlorocebus*, with *Cercopithecus* generally exhibiting narrower and more elongated upper and lower molars (Tukey's HSD *Chlorocebus* vs. *Cercopithecus* p < 0.001 in M_1^1 , M_1 , and M_3 , but p = 0.30 in M_2^2). LAET 75-3703 aligns with *Chlorocebus* in having relatively broad molars in all preserved teeth except M_1^1 (Fig. 12).

The M³ is typically distally reduced in cercopithecins, complementing the loss of the hypoconulid on M₃. The hypocone and metacone may be twinned or the metaloph may be lost altogether (e.g., Fig. 10b–c). In LAET 75-3703, the M³ is relatively small and

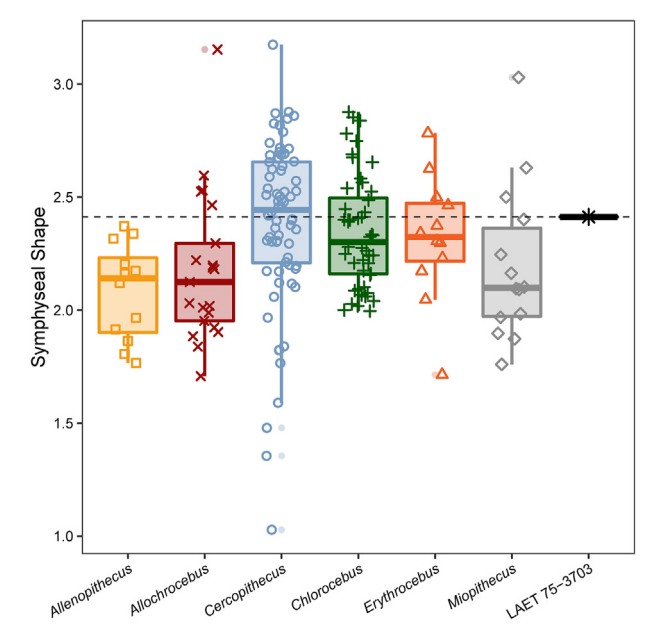


Figure 14. Boxplot of symphysis shape calculated as the superior-inferior height of the symphysis divided by the minimum anteroposterior depth of the symphysis (see Table 2 for definition of linear measurements). See also SOM Figure S3 to visualize the index as a scatterplot.

tapers distally, but the metacone and hypocone are fully developed, distinct, and connected by a complete distal loph. This is presumably a primitive retention, and it is atypical but not unique among *Chlorocebus* and *Cercopithecus* specimens. Of the specimens examined for this trait (n = 47 *Cercopithecus* and 53 *Chlorocebus*), only 16% had an unreduced or slightly reduced M^3 metaloph (23.4% of *Cercopithecus* and 9.4% of *Chlorocebus*); 13% had a substantially reduced metaloph (19.1% of *Cercopithecus* and 7.5% of *Chlorocebus*); and in 71%, the metaloph was lost (distal cusps were twinned or absent; 57.4% of *Cercopithecus* and 83.0% of *Chlorocebus*).

<u>Mandible</u> The mandible of LAET 75-3703 is typical of cercopithecines in exhibiting a short and steeply sloping symphysis, clearly marked mental ridges, and shallow mandibular corpus that is deepest anteriorly (Figs. 4 and 13). Nearly all male guenons exhibit mental ridges on the symphysis except for *Allenopithecus* and *Miopithecus*. Compared with a sample of extant cercopithecins, LAET 75-3703 has a somewhat more elongate symphysis and is closest to the means of *Cercopithecus*, *Erythrocebus*, and *Chlorocebus* in symphyseal proportions (Fig. 14; SOM Fig. S3). *Allenopithecus*, *Allochrocebus*, and *Miopithecus* have somewhat shorter or thicker symphyses on average, although these differences are not significant and only *Cercopithecus* and *Allenopithecus* are statistically distinguished from each other (ANOVA p < 0.01; Tukey's HSD *Cercopithecus* vs. *Allenopithecus* p < 0.05).

Corpus shape overlaps substantially among the guenons, although differences between some genera are statistically significant as noted previously (ANOVA p < 0.001; Gilbert et al., 2021). Allochrocebus and Miopithecus in particular have slightly shallower mandibles on average, whereas Cercopithecus spp. have relatively deeper mandibles (Tukey's HSD, Cercopithecus vs. Chlorocebus, Allochrocebus, and Miopithecus p < 0.01; Fig. 15; SOM Fig. S4). LAET 75-3703 falls closest to the mean for Cercopithecus in this index, although it is well within the range of most cercopithecin genera, including Chlorocebus (Fig. 15; SOM Fig. S4). Although broken at the level of P₄/M₁ and displaced lingually, the corpus of LAET 75-3703 is deepest anteriorly under M₁ and becomes shallower posteriorly (see arrows on Fig. 13e). This is most similar to the condition in Allenopithecus, Erythrocebus, and Chlorocebus, where the corpus is anteriorly deep and shallows posteriorly (Fig. 13; 100% of n=2Allenopithecus; 100% of n = 4 Erythrocebus; 75% of n = 52 Chlorocebus). Chlorocebus mandibles are otherwise even in depth (15%) or undulate slightly (10%; Fig. 13a). Allochrocebus mandibles tend to be even in depth (Fig. 13b; 82% of n = 11; 9% each undulating and

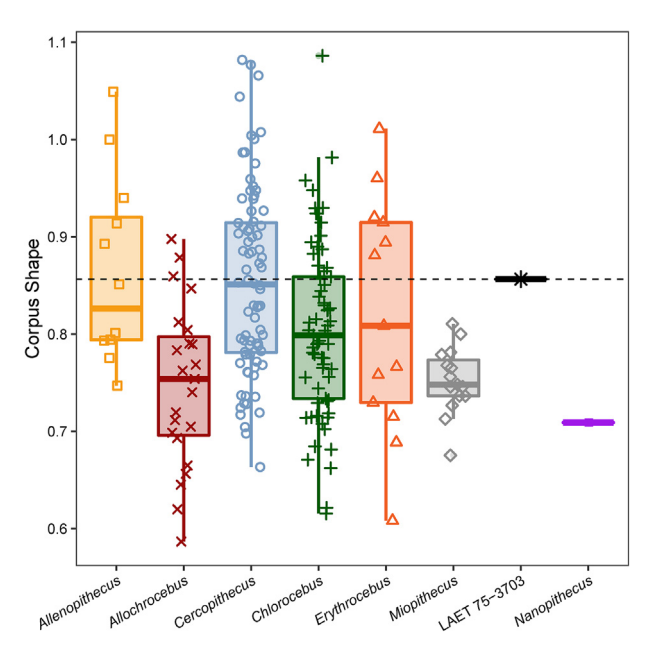


Figure 15. Boxplot of relative corpus depth, calculated as corpus depth under M_1 divided by mandibular molar row length. See also SOM Figure S4 to visualize the index as a scatterplot.

shallowing posteriorly). In contrast, the corpus in *Cercopithecus* and *Miopithecus* tend to undulate slightly along the inferior margin, such that the deepest point is below the middle of the molar row (Fig. 13c; 81% undulating, 14% even, and 5% shallowing posteriorly of n=43 *Cercopithecus*; 100% undulating of n=2 *Miopithecus*; Groves, 2000). The corpus of LAET 75-3703 lacks mandibular fossae similar to most other cercopithecins except *Allochrocebus*, which occasionally exhibit slight depressions in male mandibles. No guenons have the deeply excavated fossae seen in some papionins. The oblique line is rugose in LAET 75-3703 (Figs. 4 and 13e),

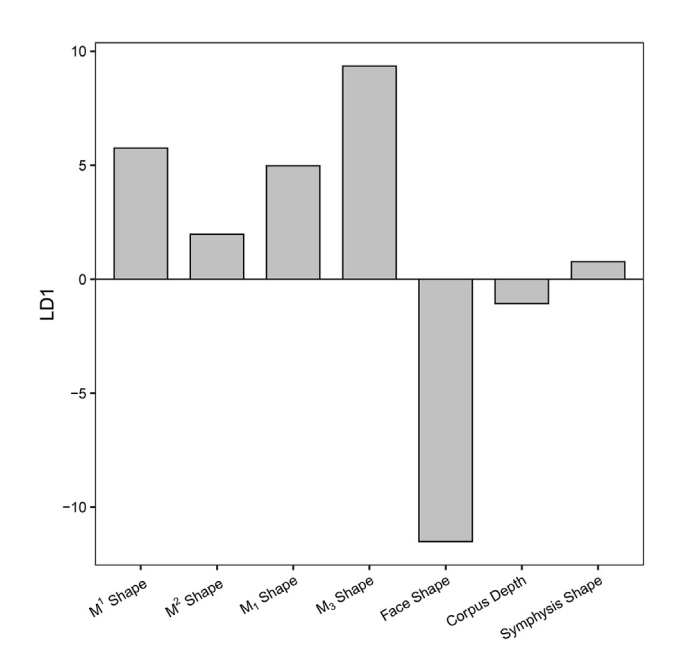


Figure 16. Loadings on the first linear discriminant vector from a discriminant function analysis (DFA) of seven indices of the face, dentition, and mandible (see Table 2) including specimens of *Chlorocebus* and *Cercopithecus* (n=92 individuals with no missing data). Molar crown shape (especially of M^1 and M_3) and face shape were the most influential variables, whereas indices of the mandible (relative corpus depth and symphysis shape) did not load strongly on LD1.

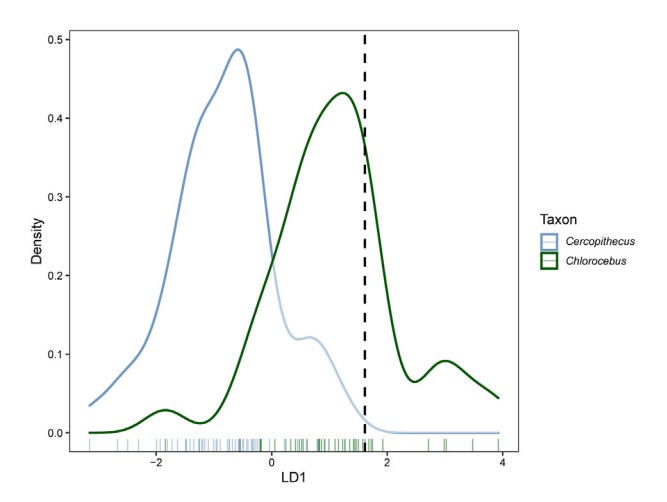


Figure 17. A density plot showing the distribution of individual values by genus along LD1. The DFA had an overall correct classification rate of 80.4%. Specimens of *Cercopithecus* and *Chlorocebus* are separated along LD1, with *Chlorocebus* falling at the positive end of the vector and *Cercopithecus* grouping at the negative end of the vector. LAET 75-3703 is represented by the vertical dashed line in the middle of the density curve for *Chlorocebus* and was classified as a member of *Chlorocebus* with a robust posterior probability of 92.7%.

forming a sharp crest similar to that seen in larger and more robust species such as *Ce. neglectus* and *Ce. mitis* (Fig. 13c) and variably in *Chlorocebus* species.

<u>Lower dentition</u> The P_3 is typical of a male cercopithecid with a single cusp and an elongated mesial honing face. The crown is buccolingually narrow as in cercopithecines generally (Delson, 1975), and it lacks the distolingual expansion commonly seen in colobines. Similar to the upper molars, the lower molars are low-crowned with rounded cusps and relatively buccolingually broad as seen in *Chlorocebus* (see above regarding the upper dentition; Fig. 12). As in the M^3 , the M_3 is only slightly reduced in LAET 75-3703, and it is relatively buccolingually broader than other sampled *Chlorocebus* taxa, including *Chlorocebus* fossil material from Asbole (single-case test, p < 0.05 against all extant species; Figs. 4 and 6c).

3.3. Multivariate analysis

The discriminant function analysis was robust with an overall correct classification rate of 80.4%, with 84.9% of Cercopithecus and 74.4% of Chlorocebus specimens classified correctly by leave-oneout cross-validation. Examination of the loadings on the linear discriminant function (LD1) shows that M¹ crown shape, M₃ crown shape, and face shape were the most influential variables, whereas aspects of the mandible (i.e., relative corpus depth and symphysis shape) were not strongly influential (Fig. 16). The loadings indicate that Chlorocebus, which clusters at the positive end of LD1, is characterized by buccolingually broader molars, a shallower and longer rostrum, and a slightly relatively elongated mandibular corpus. At the negative end of LD1, Cercopithecus is characterized by more mesiodistally elongated molars, a deeper and shorter rostrum, and a slightly deeper and shorter corpus (Figs. 16 and 17). These results are consistent with the comparisons presented earlier.

When LAET 75-3703 was included in the analysis as an unknown, the analysis classified the fossil as *Chlorocebus* with a very high posterior probability of 92.7% (represented along LD1 as the dashed vertical line in Fig. 17), consistent with its somewhat shallower and longer rostrum (Fig. 9) and buccolingually broader molars (Fig. 12).

Although the traits used in the DFA are not highly sexually dimorphic within our sample, a second analysis was performed on a sample of *Chlorocebus* and *Cercopithecus* males to assess whether sex differences were influencing the results. The results were largely similar, with an overall correct classification rate of 83.6% and with 91.2% of *Cercopithecus* and 71.4% of *Chlorocebus* specimens classified correctly following leave-one-out cross-validation. The loadings were also similar, although M² shape and relative corpus depth loaded more strongly (SOM Fig. S5). LAET 75-3703 was again classified as a member of *Chlorocebus* with 97.9% posterior probability (SOM Fig. S6).

4. Discussion

Assessing the diversity of fossil guenons has been significantly hampered by the skeletal similarity among members of the group combined with recent revisions to guenon systematics. With the recognition that the genus Cercopithecus as traditionally comprised was polyphyletic, the vervets ('C. aethiops') were removed from Cercopithecus and transferred to Chlorocebus as part of the monophyletic 'terrestrial clade' including patas monkeys (Erythrocebus) and mountain monkeys (Allochrocebus; Tosi et al., 2002b, 2004). Before this taxonomic reorganization, most Pliocene and Pleistocene material was assigned to Cercopithecus as an indicator of general cercopithecin affinity (e.g., Eck and Howell, 1972; Harrison and Harris, 1996; Jablonski et al., 2008; Jablonski and Frost, 2010). Distinguishing fossil guenon material from Cercopithecus sp. indet. (or from Cercopithecini indet. more broadly) has proven difficult with relatively few exceptions that have been able to use diagnostic features such as molar shape, incisor proportions, size, and postcranial adaptations (e.g., Frost, 2001; Frost and Alemseged, 2007; Plavcan et al., 2019). Thus, although previous taxonomic attribution of cercopithecin fossils has been largely stymied by the skeletal similarity among guenons, the completeness of the LAET 75-3703 partial skull allows a more specific attribution to the genus Chlorocebus.

Furthermore, although it is difficult to differentiate individuals of Chlorocebus and Cercopithecus based on single traits or bivariate comparisons, our analyses demonstrate that a multivariate approach assessing the cumulative signal from multiple traits is robust in distinguishing between these genera. With the possible exception of incisor proportions (Frost, 2001; Gilbert et al., 2021), Chlorocebus and Cercopithecus are instead subtly separated in several indices (e.g., orbit shape, face shape, mandibular corpus depth, molar shape) on average, and individuals are difficult to classify with confidence based on only one or two indices or features. Instead, recent morphological comparisons as well as the results presented here demonstrate the ability of multiple combined features to confidently distinguish the two genera (Frost and Alemseged, 2007; Gilbert et al., 2021). Results from our comparative study add to the still brief list of traits useful for distinguishing between the long-acknowledged skeletally similar guenons (Groves, 2000; Frost, 2001; Ravi, 2013; Gilbert et al., 2021). Our indices statistically distinguish Cercopithecus and Chlorocebus in face shape (Fig. 9), molar crown shapes (Fig. 12), and mandibular corpus shape (Fig. 15). Qualitatively, nasal aperture shape (Fig. 7), the presence of thumbprint maxillary depressions (Fig. 8), and inferior corpus margin shape (Fig. 13) are also informative in the

In some cases, our results differ from previous investigations likely because of the way these morphologies were captured. In particular, a three-dimensional (3D) geometric morphometric analysis of guenon cranial shape suggested *Chlorocebus* exhibited a relatively longer face than *Cercopithecus*, similar to our findings (Cardini and Elton, 2008). Conversely, Gilbert et al. (2021) found facial length was relatively longer in *Cercopithecus*, but this was calculated as the length of the entire face (nasion—prosthion) relative to neurocranial length. It is possible that the index used

here, specifically lower face length relative to midfacial depth, captured morphology more similar to that captured by the analyses of Cardini and Elton (2008) than the index used by Gilbert et al. (2021). Additionally, although we also detected a significant difference in mandibular corpus depth between Chlorocebus and Cercopithecus, we find more overlap in corpus shape than did Gilbert et al. (2021), who calculated corpus depth relative to a different measure of overall mandibular size. Such variation in the degree or direction of separation dependent on how the morphology is quantified underscores how subtle these morphological differences can be and again highlights the importance of assessing multiple features together and, where possible, using large sample sizes to enhance the detection of these differences. However, the overall consistent signal among these features (e.g., relative lower facial length, orbit shape, mandibular corpus depth) across studies and across methodologies suggests they represent real distinctions between guenon genera and that further investigations will likely uncover additional informative metrics. In sum, the results presented here provide compelling support for assigning LAET 75-3703 to Chlorocebus. In particular, LAET 75-3703 shares exclusively with Chlorocebus the following combination of features: 1) small, shallow, bounded 'thumbprint' depressions on the maxilla; 2) a tall, narrow, and diamond-shaped nasal aperture; 3) squarer and less mesiodistally elongated molars; and 4) a shallow mandible that decreases in depth posteriorly. The DFA results also strongly supported the attribution of LAET 75-3703 to Chlorocebus and highlighted shared indices of face shape and molar crown shape. Although sample sizes of other guenon genera with no missing data were too small to be included in the DFA, several morphological features distinguish LAET 75-3703 from Allenopithecus, Allochrocebus, Erythrocebus, and Miopithecus, including molar crown shapes, dorsal rostral shape, and nasal aperture shape (see Subsection 3.2.). In addition, LAET 75-3703 is distinguished from all sampled extant and fossil guenons, including Chlorocebus species, in the presence of an extremely small P³ relative to M¹ size (Figs. 3f and 11), warranting its status as a new species, Ch. ngedere. At ~1.7–1.2 Ma, Ch. ngedere is the oldest fossil representative of Chlorocebus and the oldest definitive representative of a modern cercopithecin genus (Fig. 2).

Chlorocebus includes all of the forms previously considered subspecies of C. aethiops, characterized by their medium body size, semiterrestrial postcranial adaptations, and general ecological flexibility, now usually recognized as six to seven distinct species (Lernould, 1988; Groves, 1989, 2001; Grubb et al., 2003; Groves and Kingdon, 2013; Kingdon, 2015; Lo Bianco et al., 2017; Turner et al., 2019b). They are phenotypically and genetically distinct despite ongoing hybridization and relatively recent estimated divergence times (Cardini et al., 2007; Groves and Kingdon, 2013; Svardal et al., 2017; Detwiler, 2019; van der Valk et al., 2020), paralleling the situation in Papio (e.g., Jolly, 1993; Groves, 2001; Frost et al., 2003; Kamilar, 2006; Zinner et al., 2013; Warren et al., 2015; Dolotovskaya et al., 2017; Gilbert et al., 2018). Following these more recent studies, we adhere to a phylogenetic species concept (PSC) in this study and rely on consistent phenotypic differences instead of reproductive isolation as our criteria for recognizing distinct or separate evolutionary lineages in the fossil record. By that measure, the phenotypic differences seen in Ch. ngedere, particularly the small P³ outside the known range of variation seen in any sample of extant or fossil Chlorocebus specimens, are distinct enough in our view to justify the recognition of a new species using a PSC. In the case of a single specimen, one must generally assume that the specimen exhibits morphology close to the population mean for most features, as that is the most statistically likely scenario. Our single-case tests formalize these assumptions and demonstrate Ch. ngedere is almost certainly distinct from all other sampled

populations, thereby strongly supporting its classification as a new species under a PSC.

The estimated Early Pleistocene age of Ch. ngedere is well within the projected time range of the origin of crown Chlorocebus to the exclusion of Ch. dryas at ~3.5-1 Ma (95% composite CI: 3.91-0.7 Ma; Springer et al., 2012; Dolotovskaya et al., 2017; van der Valk et al., 2020). Recently, the enigmatic dryas monkey was confirmed to be the sister of other Chlorocebus species rather than aligned with Cercopithecus on the basis of molecular and morphological data (van der Valk et al., 2020; Gilbert et al., 2021), reinforcing the suggestions of some earlier studies (Kuroda et al., 1985; Guschanski et al., 2013). However, Ch. dryas is morphologically and ecologically distinct from the other Chlorocebus species and may ultimately belong to a new genus (Kuroda et al., 1985; Butynski, 2013; Hart et al., 2019; Alempijevic et al., 2021; Gilbert et al., 2021). The species-level relationships within *Chlorocebus* are not yet fully resolved, and likely as a result of historical and ongoing hybridization, different datasets recover different topologies (Fig. 1; Perelman et al., 2011; Springer et al., 2012; Guschanski et al., 2013; Haus et al., 2013; Svardal et al., 2017; van der Valk et al., 2020). Dolotovskaya et al. (2017) proposed that the basal-most branching of the West African Ch. sabaeus suggests an origin for the genus north of the central African rainforest, with modern vervet lineages appearing separately in eastern Africa at ca. 2.12 Ma (95% HPD, 2.42-1.83 Ma) and again at ca. 1.81 Ma (95% HPD, 2.0-1.61 Ma). Other members of the terrestrial guenon clade, Erythrocebus and Allochrocebus, are also found today in central and western Africa (Butynski et al., 2013).

Regardless of the position of Ch. ngedere within the Chlorocebus clade, its similarity to the living members of the genus (excluding Ch. dryas) suggests that its ecological adaptations would likely have been broadly similar. It overlaps with larger males in nearly all metrics, suggesting a similar body size (Fig. 6a-b; SOM Tables S2-S5). Today, Chlorocebus has a wide geographic distribution and ecological tolerance (Kingdon, 2015; Turner et al., 2019b). Extant Ch. pygerythrus is found in the Laetoli area and occurs primarily in acacia woodland along river courses (Groves and Kingdon, 2013; Kingdon, 2015). However, as Plavcan et al. (2019) noted, modern distributions of taxa do not necessarily predict the ecology or biogeography of extinct populations. Data for inferring the paleoecology of the LNB directly are scanty, but the composition of the ungulate fauna points to a predominance of open woodland and grassland habitats during the later Pleistocene. Evidence from stream channels and the coarse-grained nature of the fluvial sediments in the LNB indicates a relatively well-watered environment (Hay, 1987). This is supported by the occurrence of H. gorgops, which represents the earliest (and only) occurrence of a hippopotamid in the Laetoli sequence (T.H., pers. obs.).

The limited fossil record of guenons is somewhat surprising given their modern abundance and diversity in African ecosystems (Grubb et al., 2003; Tosi et al., 2005; Xing et al., 2007; Butynski et al., 2013). The scantiness of the cercopithecin fossil record has been explained either as a product of sampling bias, in that forestdwelling small-bodied mammals are generally under-represented in the fossil record, or as a marker of their genuine rarity (Eck and Howell, 1972; Eck, 1987; Leakey, 1988; Jablonski et al., 2008). Cercopithecins are rare even at sites that yield abundant papionin and colobine fossils, including forms attributed to more arboreal taxa such as Lophocebus and Colobus, as well as abundant micromammals (Eck, 1977, 1987; Kalb et al., 1982a; Leakey, 1988; Jablonski et al., 2008). Furthermore, a reassessment of the evolution of cercopithecin positional behavior suggests that the earliest guenons were more likely semiterrestrial than arboreal (Arenson et al., 2020), so ecological biases may not entirely explain the paucity of early cercopithecin fossils. Cercopithecins were probably

a genuinely rare component of the primate fauna until their diversification in the later Pleistocene. Such a scenario is consistent with extant evidence of ongoing speciation and hybridization among the living guenon populations, which is likewise suggestive of their recent diversification (e.g., Detwiler et al., 2005; Springer et al., 2012; Guschanski et al., 2013; Lo Bianco et al., 2017). The recovery of new fossil specimens from Plio-Pleistocene sites in Africa, as well as the study of existing collections from paleontological sites such as those from Laetoli, will help better document taxonomic diversity in the guenon fossil record. Furthermore, some of the morphological features noted here, as well as in other recent analyses (Groves, 2000; Frost, 2001; Frost and Alemseged, 2007; Arenson et al., 2020; Gilbert et al., 2021), may prove useful in assigning fossil guenon specimens to more specific taxonomic ranks in the future.

5. Conclusions

Guenon fossils are exceptionally scarce relative to the diversity of the modern radiation, but recent finds have begun to expand the geographic and taxonomic range of the known fossil record (e.g., Gilbert et al., 2014; Plavcan et al., 2019; Frost et al., 2020). The description of a partial skull from the Early Pleistocene of Laetoli represents one of the most complete specimens in a fossil record largely represented by fragmentary dentognathic remains. It allows us to confidently attribute LAET 75-3703 to Chlorocebus and describe a new species, Ch. ngedere, on the basis of its uniquely small P³. Several diagnostic features and indices of the lower face. mandible, and dentition were examined with a large comparative sample of extant guenons. A DFA separates the skeletally similar Chlorocebus and Cercopithecus with strong statistical support and confidently classifies LAET 75-3703 as Chlorocebus. As the first record of a cercopithecin from the site of Laetoli and the oldest fossil confidently attributed to a modern genus (Fig. 2), Ch. ngedere represents a significant addition to the guenon fossil record.

Declaration of competing interest

The authors declare no conflict of interest impacting the work presented in this paper.

Acknowledgments

Research in Tanzania and access to fossil collections was granted by the Tanzania Commission for Science and Technology, the Department of Antiquities, and the National Museum of Tanzania. We thank the following curators and collection managers for access to collections in their care: Amandus Kweka and Agness Gidna, National Museum of Tanzania, Dar es Salaam; Job Kibii, Jimmy Yatich, and Justus Erus, National Museum of Kenya, Nairobi; Neil Duncan, Eleanor Hoeger, Marisa Surovy, and Sara Ketelsen, Department of Mammalogy, American Museum of Natural History, New York; Adam Ferguson and Lauren Smith, Department of Mammals, Field Museum of Natural History, Chicago; Darrin Lunde, Division of Mammals, United States National Museum of Natural History, Smithsonian Institution, Washington D.C; Emmanuel Gilissen and Wim Wendelen, Royal Museum for Central Africa, Tervuren, Belgium; Mark Omura, Department of Mammalogy, Harvard University Museum of Comparative Zoology, Cambridge; and Malcolm Harman, the Powell-Cotton Museum, Birchington-on-Sea, United Kingdom. We thank Eric Delson and colleagues for access to the NYCEP PRImate Morphometrics Online (PRIMO) database. We also thank Emma Curtis for help with data collection. Finally, we thank Clément Zanolli, David Alba, and three anonymous reviewers for their detailed and helpful comments, which

have improved this manuscript. Photographs of Museum of Comparative Zoology specimens are copyrighted by the President and Fellows of Harvard College. This study was generously supported by the National Science Foundation (IGERT #0333415 [NYCEP], GRFP Award #40F79-02 04, #BCS-2018093, #BCS-0309513, #BCS-0216683 and #BSC-1350023), the American Association of Physical Anthropologists Professional Development Grant Program, the PSC-CUNY Faculty Research Award Program (Award #60347-00 48), and the Hunter College Presidential Travel Award Program.

Supplementary Online Material

Supplementary Online Material related to this article can be found at https://doi.org/10.1016/j.jhevol.2021.103136.

References

- Alempijevic, D., Boliabo, E.M., Coates, K.F., Hart, T.B., Hart, J.A., Detwiler, K.M., 2021.
 A natural history of *Chlorocebus dryas* from camera traps in Lomami National Park and its buffer zone, Democratic Republic of the Congo, with notes on the species status of *Cercopithecus salongo*. Am. J. Primatol. 83, e23261.
- Alemseged, Z., Geraads, D., 2000. A new middle Pleistocene fauna from the busidima—Telalak region of the Afar, Ethiopia. C. R. Acad. Sci. Paris 331, 549—556.
- Arenson, J.L., Sargis, E.J., Hart, J.A., Hart, T.B., Detwiler, K.M., Gilbert, C.C., 2020. Skeletal morphology of the lesula (*Cercopithecus lomamiensis*) and the evolution of guenon locomotor behavior. Am. J. Phys. Anthropol. 172, 3–24.
- Assefa, Z., 2006. Faunal remains from Porc-epic: Paleoecological and zooarchaeological investigations from a middle stone age site in southeastern Ethiopia. J. Hum. Evol. 51, 50–75.
- Broadfield, D.C., Delson, E., Atsalis, S., 1994. Cercopithecid fossils from the later Pleistocene of Taung, South Africa. Am. J. Phys. Anthropol. 37, 59–60.
- Butynski, T.M., 2002. The guenons: An overview of diversity and taxonomy. In: Glenn, M.E., Cords, M. (Eds.), The Guenons: Diversity and Adaptation in African Monkeys. Plenum Publishers, New York, pp. 3–13.
- Butynski, T.M., 2013. *Cercopithecus dryas* Dryad monkey (Salongo monkey). In:
 Butynski, T.M., Kingdon, J., Kalina, J. (Eds.), Mammals of Africa: Volume II:
 Primates. Bloomsbury Publishing, London, pp. 306–309.
- Butynski, T.M., Kingdon, J., Kalina, J. (Eds.), 2013. Mammals of Africa. Volume II: Primates. Bloomsbury Publishing, London.
- Cardini, A., Elton, S., 2008. Variation in guenon skulls (I): Species divergence, ecological and genetic differences. J. Hum. Evol. 54, 615–637.
- Cardini, A., Jansson, A.-U., Elton, S., 2007. A geometric morphometric approach to the study of ecogeographical and clinal variation in vervet monkeys. J. Biogeogr. 34, 1663—1678.
- Deino, A.L., 2011. 40Ar/39Ar dating of Laetoli, Tanzania. In: Harrison, T. (Ed.), Pale-ontology and Geology of Laetoli: Human Evolution in Context. Vol. 1: Geology, Geochronology, Paleoecology, and Paleoenvironment. Springer, Dordrecht, pp. 77—97.
- Deino, A.L., Heil Jr., C., King, J., McHenry, L.J., Stanistreet, I.G., Stollhofen, H., Njau, J.K., Mwankunda, J., Schick, K., Toth, N., 2021. Chronostratigraphy and age modeling of Pleistocene drill cores from the Olduvai basin, Tanzania (Olduvai Gorge coring project). Palaeogeogr. Palaeoclimatol. Palaeoecol. 571, 109990.
- Delson, E., 1973. Fossil colobine monkeys of the Circum-Mediterranean region and the evolutionary history of the Cercopithecidae (Primates, Mammalia). Ph.D. Dissertation. Columbia University.
- Delson, E., 1975. Evolutionary history of the Cercopithecidae. In: Szalay, F.S. (Ed.), Approaches to Primate Paleobiology. Karger, Basel, pp. 167–217.
- Detwiler, K.M., 2019. Mitochondrial DNA analyses of *Cercopithecus* monkeys reveal a localized hybrid origin for *C. mitis doggetti* in Gombe National Park, Tanzania. Int. J. Primatol. 40, 28–52.
- Detwiler, K.M., Burrell, A.S., Jolly, C.J., 2005. Conservation implications of hybridization in African cercopithecine monkeys. Int. J. Primatol. 26, 661–684.
- Dietrich, W.O., 1942. Altestquartäre Säugetiere aus der Südlichen Serengeti, Deutsch-Ostafrika. Palaeontographica 94, 43–133.
- Dolotovskaya, S., Torroba Bordallo, J., Haus, T., Noll, A., Hofreiter, M., Zinner, D., Roos, C., 2017. Comparing mitogenomic timetrees for two African savannah primate genera (*Chlorocebus* and *Papio*). Zool. J. Linn. Soc. 181, 471–483.
- Drake, R., Curtis, G.H., 1978. K-Ar geochronology of the Laetoli fossil localities. In: Leakey, M.D., Harris, J.M. (Eds.), Laetoli: A Pliocene Site in Northern Tanzania. Oxford University Press, Oxford, pp. 48–52.
- Eck, G.G., 1977. Diversity and frequency distribution of Omo group Cercopithecoidea. J. Hum. Evol. 6, 55–63.
- Eck, G.G., 1987. Plio-pleistocene specimens of Cercopithecus from the Shungura formation, southwestern Ethiopia. In: Coppens, Y., Howell, F.C. (Eds.), Les Faunes Plio-Pléistocènes de La Basse Vallée de l'Omo (Éthiopie). Tome 3, Cercopithecidae de La Formation de Shungura. Cahiers de Paleontologie, Travaux de Paléontologie Est-Africaine, CNRS, Paris, pp. 143–146.

- Eck, G.G., Howell, F.C., 1972. New fossil *Cercopithecus* material from the lower Omo Basin, Ethiopia. Folia Primatol. 18, 325—355.
- Fabre, P.-H., Rodrigues, A., Douzery, E.J.P., 2009. Patterns of macroevolution among Primates inferred from a supermatrix of mitochondrial and nuclear DNA. Mol. Phylogenet. Evol. 53, 808–825.
- Frost, S.R., 2001. Fossil Cercopithecidae of the Afar Depression, Ethiopia: Species systematics and comparison to the Turkana Basin. Ph.D. Dissertation. The City University of New York.
- Frost, S.R., Alemseged, Z., 2007. Middle Pleistocene fossil Cercopithecidae from Asbole, Afar region, Ethiopia. J. Hum. Evol. 53, 227–259.
- Frost, S.R., Marcus, L.F., Bookstein, F.L., Reddy, D.P., Delson, E., 2003. Cranial allometry, phylogeography, and systematics of large-bodied papionins (Primates: Cercopithecinae) inferred from geometric morphometric analysis of landmark data. Anat. Rec. 275A, 1048–1072.
- Frost, S.R., Gilbert, C.C., Delson, E., 2018. Review of Cercopithecidae from upper Laetolil beds, Tanzania, indicates presence of *Theropithecus*: Biogeographic and taxonomic implications. Am. J. Phys. Anthropol. 165, 90–91
- Frost, S.R., Ward, C.V., Manthi, F.K., Plavcan, J.M., 2020. Cercopithecid fossils from Kanapoi, west Turkana, Kenya (2007–2015). J. Hum. Evol. 140, 102642.
- Geoffroy Saint-Hilaire, É., 1812. Tableau des Quadrumanes, 1. Ord. Quadrumanes. Ann. Muséum Hist. Nat. Paris. 19, 85–122.
- Gilbert, C.C., Bibi, F., Hill, A., Beech, M.J., 2014. Early guenon from the late Miocene Baynunah Formation, Abu Dhabi, with implications for cercopithecoid biogeography and evolution. Proc. Natl. Acad. Sci. USA 111, 10119—10124.
- Gilbert, C.C., Frost, S.R., Pugh, K.D., Anderson, M., Delson, E., 2018. Evolution of the modern baboon (*Papio hamadryas*): A reassessment of the African Plio-Pleistocene record. J. Hum. Evol. 122, 38–69.
- Gilbert, C.C., Gilissen, E., Arenson, J.L., Patel, B.A., Nakatsukasa, M., Hart, T.B., Hart, J.A., Detwiler, K.M., Sargis, E.J., 2021. Morphological analysis of new Dryas monkey specimens from the Central Congo Basin: Taxonomic considerations and an emended diagnosis. Am. J. Phys. Anthropol. 176, 361–389.
- Gray, J.E., 1821. On the natural arrangement of vertebrose animals. Lond. Med. Repos. 15, 296–310.
- Gray, J.E., 1870. Catalogue of Monkeys, Lemurs, and Fruit-Eating Bats in the Collection of the British Museum. British Museum of Natural History, London.
- Groves, C.P., 1989. A Theory of Human and Primate Evolution. Oxford University Press, Oxford.
- Groves, C.P., 2000. The phylogeny of the Cercopithecoidea. In: Whitehead, P.F., Jolly, C.J. (Eds.), Old World Monkeys. Cambridge University Press, Cambridge, pp. 180–213.
- Groves, C.P., 2001. Primate Taxonomy. Smithsonian, Washington.
- Groves, C.P., Kingdon, J., 2013. Genus Chlorocebus. In: Butynski, T.M., Kingdon, J., Kalina, J. (Eds.), Mammals of Africa: Volume II: Primates. Bloomsbury Publishing, London, pp. 264–266.
- Grubb, P., Butynski, T.M., Oates, J.F., Bearder, S.K., Disotell, T.R., Groves, C.P., Struhsaker, T.T., 2003. Assessment of the diversity of African primates. Int. J. Primatol. 24, 1301–1357.
- Guschanski, K., Krause, J., Sawyer, S., Valente, L.M., Bailey, S., Finstermeier, K., Sabin, R., Gilissen, E., Sonet, G., Nagy, Z.T., Lenglet, G., Mayer, F., Savolainen, V., 2013. Next-generation museomics disentangles one of the largest primate radiations. Syst. Biol. 62, 539–554.
- Harris, J.W.K., Harris, K., 1981. A note on the archaeology of Laetoli. Nyame Akuma 18, 18–21
- Harrison, T., 2011. Cercopithecids (Cercopithecidae, primates). In: Harrison, T. (Ed.), Paleontology and Geology of Laetoli: Human Evolution in Context. Vol. 2: Fossil Hominins and the Associated Fauna. Springer, Dordrecht, pp. 83–139.
- Harrison, T., Harris, E.E., 1996. Plio-pleistocene cercopithecids from Kanam East, western Kenya. J. Hum. Evol. 30, 539–561.
- Harrison, T., Kweka, A., 2011. Paleontological localities on the Eyasi plateau, including Laetoli. In: Harrison, T. (Ed.), Paleontology and Geology of Laetoli: Human Evolution in Context. Vol. 1: Geology, Geochronology, Paleoecology, and Paleoenvironment. Springer, Dordrecht, pp. 17–45.
- Hart, J.A., Detwiler, K.M., Alempijevic, D., Lokasola, A., Rylands, A.B., 2019. Cercopithecus dryas. The IUCN Red List of Threatened Species 2019: e.T4216A17947691.
- Haus, T., Akom, E., Agwanda, B., Hofreiter, M., Roos, C., Zinner, D., 2013. Mito-chondrial diversity and distribution of African green monkeys (*Chlorocebus* Gray, 1870). Am. J. Primatol. 75, 350–360.
- Hay, R.L., 1987. Geology of the Laetoli area. In: Leakey, M.D., Harris, J.M. (Eds.), Laetoli: A Pliocene Site in Northern Tanzania. Oxford University Press, Oxford, pp. 23–47.
- Jablonski, N.G., Frost, S.R., 2010. Cercopithecoidea. In: Werdelin, L., Sanders, W.J. (Eds.), The Cenozoic Mammals of Africa. University of California Press, Berkeley, pp. 393–428.
- Jablonski, N.G., Leakey, M.G., Antón, M., 2008. Systematic paleontology of the cercopithecines. In: Jablonski, N.G., Leakey, M.G. (Eds.), Koobi Fora Research Project: Volume 6. The Fossil Monkeys. California Academy of Sciences, San Francisco, pp. 103–238.
- Jolly, C.J., 1993. Species, subspecies, and baboon systematics. In: Kimbel, W.H., Martin, L.B. (Eds.), Species, Species Concepts, and Primate Evolution. Plenum Press, New York, pp. 67–107.
- Kalb, J.E., Jolly, C.J., Mebrate, A., Tebedge, S., Smart, C., Oswald, E.B., Cramer, D., Whitehead, P., Wood, C.B., Conroy, G.C., Adefris, T., Sperling, L., Kana, B., 1982a. Fossil mammals and artefacts from the middle Awash valley, Ethiopia. Nature 298, 25–29.

- Kalb, J.E., Oswald, E.B., Tebedge, S., Mebrate, A., Tola, E., Peak, D., 1982b. Geology and stratigraphy of Neogene deposits, middle Awash valley, Ethiopia. Nature 298, 17—25.
- Kamilar, J.M., 2006. Geographic variation in savanna baboon (*Papio*) ecology and its taxonomic and evolutionary implications. In: Lehman, S.M., Fleagle, J.G. (Eds.), Primate Biogeography. Springer, New York, pp. 169–200.
- Kassambara, A., 2020. ggpubr: "ggplot2" Based Publication Ready Plots., R package version 0.2.5. https://CRAN.R-project.org/package=ggpubr.
- Kingdon, J., 2015. The Kingdon Field Guide to African Mammals, 2nd ed. Bloomsbury Publishing. London.
- Klein, R.G., 1977. The mammalian fauna from the Middle and Later Stone Age (later Pleistocene) levels of Border Cave, Natal Province, South Africa. S. Afr. Archaeol. Bull. 32. 14–27.
- Kohl-Larsen, L., 1943. Auf den Spuren des Vormenschen. Forshungen, Fahrten und Erlebnisse in Deutsch-Ostafrika, 2nd Band. Strecker und Schröder, Stuttgart.
- Kuroda, S., Kano, T., Muhindo, K., 1985. Further information on the new monkey species, *Cercopithecus salongo* Thys van den Audenaerde, 1977. Primates 26, 325–333.
- Laird, M.F., Kozma, E.E., Kwekason, A., Harrison, T., 2018. A new fossil cercopithecid tibia from Laetoli and its implications for positional behavior and paleoecology. J. Hum. Evol. 118, 27–42.
- Lampel, G., 1963. Variationsstatistische und morphologische Untersuchungen am Gebiß der Cercopithecinen. Acta Anat. 49, 1–122.
- Leakey, M.G., 1976. Cercopithecoidea of the East Rudolf succession. In: Coppens, Y., Howell, F.C., Isaac, G.L., Leakey, R.E.F. (Eds.), Earliest Man and Environments in the Lake Rudolf Basin. University of Chicago Press, Chicago, pp. 345–350.
- Leakey, M.D., 1987. Introduction. In: Leakey, M.D., Harris, J.M. (Eds.), Laetoli: A Pliocene Site in Northern Tanzania. Oxford University Press, Oxford, pp. 1–22.
- Leakey, M.G., 1988. Fossil evidence for the evolution of the guenons. In: Gautier-Hion, A., Bourliere, F., Gautier, J.-P., Kingdon, J. (Eds.), A Primate Radiation: Evolutionary Biology of the African Guenons. Cambridge University Press, Cambridge, pp. 7–12.
- Leakey, M.G., Delson, E., 1987. Fossil Cercopithecidae from the Laetolil beds. In: Leakey, M.D., Harris, J.M. (Eds.), Laetoli: A Pliocene Site in Northern Tanzania. Oxford University Press, Oxford, pp. 91–107.
- Lernould, J.-M., 1988. Classification and geographical distribution of guenons: A review. In: Gautier-Hion, A., Bourliere, F., Gautier, J.-P., Kingdon, J. (Eds.), A Primate Radiation: Evolutionary Biology of the African Guenons. Cambridge University Press, Cambridge, pp. 54–78.
- Linden, B., Dalton, D.L., Ralph, T.M., Silva, I., Kotze, A., Taylor, P.J., 2020. Adding another piece to the southern African *Cercopithecus* monkey phylogeography puzzle. Afr. Zool. 55, 351–362.
- Linnaeus, C., 1758. Systema Naturae per Regna Tria Naturae, secundum Classes, Ordines Genera, Species cum Characteribus, Differentis, Synonymis, Locis. Edito Decima, Reformata. Laurentii Salvii, Stockholm.
- Lo Bianco, S., Masters, J.C., Sineo, L., 2017. The evolution of the Cercopithecini: A (post)modern synthesis. Evol. Anthropol. 26, 336–349.
- Manega, P., 1993. Geochronology, geochemistry, and isotopic study of the Plio-Pleistocene hominid sites and the Ngorongora volcanic highlands in northern Tanzania. Ph.D. Dissertation. University of Colorado at Boulder.
- Mokokwe, D.W., 2016. Taxonomy, taphonomy and spatial distribution of the cercopithecoid postcranial fossils from Sterkfontein caves. Ph.D. Dissertation. University of Witwatersrand.
- Ndessokia, P.N.S., 1990. The mammalian fauna and archaeology of the Ndolanya and Olpiro Beds, Laetoli, Tanzania. Ph.D. Dissertation. University of California.
- Ogola, C.A., 2009. The Sterkfontein western breccias: Stratigraphy, fauna, and artefacts. Ph.D. Dissertation. University of the Witwatersrand.
- Perelman, P., Johnson, W.E., Roos, C., Seuánez, H.N., Horvath, J.E., Moreira, M.A.M., Kessing, B., Pontius, J., Roelke, M., Rumpler, Y., Schneider, M.P.C., Silva, A., O'Brien, S.J., Pecon-Slattery, J., 2011. A molecular phylogeny of living primates. PLoS Genet. 7, e1001342.
- Plavcan, J.M., Ward, C.V., Kay, R.F., Manthi, F.K., 2019. A diminutive Pliocene guenon from Kanapoi, west Turkana, Kenya. J. Hum. Evol. 135, 102623.
- Prendergast, M.E., Luque, L., Domínguez-Rodrigo, M., Diez-Martín, F., Mabulla, A.Z.P., Barba, R., 2007. New excavations at Mumba Rockshelter, Tanzania. J. Afr. Archaeol. 5, 217–243.
- R Core Team, 2018. R: A language and environment for statistical computing. R Foundation for Statistical Computing, Vienna.

- Raaum, R.L., Sterner, K.N., Noviello, C.M., Stewart, C.-B., Disotell, T.R., 2005. Catarrhine primate divergence dates estimated from complete mitochondrial genomes: Concordance with fossil and nuclear DNA evidence. J. Hum. Evol. 48, 237–257.
- Ravi, S., 2013. Craniodental morphological evolution of the African guenons (Tribe Cercopithecini). MSc. Thesis. Hunter College, The City University of New York.
- Reed, D., Harrison, T., Kwekason, A., 2019. Eyasi plateau paleontological expedition, Laetoli, Tanzania, fossil specimen database 1998–2005. Sci. Data. 6, 304.
- Sokal, R.R., Rohlf, F.J., 1995. Biometry, 3rd ed. W. H. Freedman and Co., New York. Springer, M.S., Meredith, R.W., Gatesy, J., Emerling, C.A., Park, J., Rabosky, D.L., Stadler, T., Steiner, C., Ryder, O.A., Janečka, J.E., Fisher, C.A., Murphy, W.J., 2012. Macroevolutionary dynamics and historical biogeography of primate diversifi-
- cation inferred from a species supermatrix. PLoS One 7, e49521.

 Steiper, M.E., Young, N.M., 2006. Primate molecular divergence dates. Mol. Phylogenet. Evol. 41, 384–394.
- Svardal, H., Jasinska, A.J., Apetrei, C., Coppola, G., Huang, Y., Schmitt, C.A., Jacquelin, B., Ramensky, V., Müller-Trutwin, M., Antonio, M., Weinstock, G., Grobler, J.P., Dewar, K., Wilson, R.K., Turner, T.R., Warren, W.C., Freimer, N.B., Nordborg, M., 2017. Ancient hybridization and strong adaptation to viruses across African vervet monkey populations. Nat. Genet. 49, 1705–1713.
- Szalay, F.S., Delson, E., 1979. Evolutionary history of the primates. Academic Press, New York
- Tosi, A.J., Buzzard, P.J., Morales, J.C., Melnick, D.J., 2002a. Y-chromosome data and tribal affiliations of *Allenopithecus* and *Miopithecus*. Int. J. Primatol. 23, 1287–1299
- Tosi, A.J., Buzzard, P.J., Morales, J.C., Melnick, D.J., 2002b. Y-chromosomal window onto the history of terrestrial adaptation in the Cercopithecini. In: Glenn, M.E., Cords, M. (Eds.), The Guenons: Diversity and Adaptation in African Monkeys. Kluwer Academic Publishers, New York, pp. 13—24.
- Tosi, A.J., Melnick, D.J., Disotell, T.R., 2004. Sex chromosome phylogenetics indicate a single transition to terrestriality in the guenons (tribe Cercopithecini). J. Hum. Evol. 46, 223–237.
- Tosi, A.J., Detwiler, K.M., Disotell, T.R., 2005. X-chromosomal window into the evolutionary history of the guenons (Primates: Cercopithecini). Mol. Phylogenet. Evol. 36, 58–66.
- Turner, T.R., Schmitt, C.A., Cramer, J.D., 2019a. Savanna monkey taxonomy. In: Turner, T.R., Schmitt, C.A., Cramer, J.D. (Eds.), Savanna Monkeys: The Genus *Chlorocebus*. Cambridge University Press, Cambridge, pp. 31–54.
- Turner, T.R., Schmitt, C.A., Cramer, J.D., 2019b. Behavioral ecology of savanna monkeys. In: Turner, T.R., Schmitt, C.A., Cramer, J.D. (Eds.), Savanna Monkeys: The Genus *Chlorocebus*. Cambridge University Press, Cambridge, pp. 109–126.
- van der Valk, T., Gonda, C.M., Silegowa, H., Almanza, S., Sifuentes-Romero, I., Hart, T.B., Hart, J.A., Detwiler, K.M., Guschanski, K., 2020. The genome of the endangered Dryas monkey provides new insights into the evolutionary history of the vervets. Mol. Biol. Evol. 1–12.
- Venables, W.N., Ripley, B.D., 2002. Modern Applied Statistics with S, 4th ed. Springer, New York.
- Verheyen, W.N., 1962. Contribution à la craniologie comparée des primates: Les genres Colobus Illiger 1811 et Cercopithecus Linné 1758. Ann. Sci. Zool. Mus. R. Afr. Cent. 105, 1–247.
- Warren, W.C., Jasinska, A.J., García-Pérez, R., Svardal, H., Tomlinson, C., Rocchi, M., Archidiacono, N., Capozzi, O., Minx, P., Montague, M.J., Kyung, K., Hillier, L.W., Kremitzki, M., Graves, T., Chiang, C., Hughes, J., Tran, N., Huang, Y., Ramensky, V., Choi, O., Jung, Y.J., Schmitt, C.A., Juretic, N., Wasserscheid, J., Turner, T.R., Wiseman, R.W., Tuscher, J.J., Karl, J.A., Schmitz, J.E., Zahn, R., O'Connor, D.H., Redmond, E., Nisbett, A., Jacquelin, B., Müller-Trutwin, M.C., Brenchley, J.M., Dione, M., Antonio, M., Schroth, G.P., Kaplan, J.R., Jorgensen, M.J., Thomas, G.W.C., Hahn, M.W., Raney, B.J., Aken, B., Nag, R., Schmitz, J., Churakov, G., Noll, A., Stanyon, R., Webb, D., Thibaud-Nissen, F., Nordborg, M., Marques-Bonet, T., Dewar, K., Weinstock, G.M., Wilson, R.K., Freimer, N.B., 2015. The genome of the vervet (Chlorocebus aethiops sabaeus). Genome Res. 25, 1921–1933.
- Wickham, H., 2016. ggplot2: Elegant Graphics for Data Analysis. Springer-Verlag, New York.
- Xing, J., Wang, H., Zhang, Y., Ray, D.A., Tosi, A.J., Disotell, T.R., Batzer, M.A., 2007. A mobile element-based evolutionary history of guenons (tribe Cercopithecini). BMC Biol. 5, 1–10.
- Zinner, D., Wertheimer, J., Liedigk, R., Groeneveld, L.F., Roos, C., 2013. Baboon phylogeny as inferred from complete mitochondrial genomes. Am. J. Phys. Anthropol. 150, 133–140.